Late Pleistocene regional extension rate derived from earthquake geology of late Quaternary faults across the Great Basin, Nevada, between 38.5°N and 40°N latitude

Rich D. Koehler[†] **and Steve G. Wesnousky**
Center for Neotectonic Studies, University of Nevada–Reno, Reno, Nevada 89557, USA

ABSTRACT

Maps showing Quaternary deposits and active fault traces, paleoseismic trenches, scarp diffusion analyses, and soil characteristics in displaced alluvial surfaces are combined with previous paleoseismic studies to examine the character of late Pleistocene earthquake recurrence and estimate the net extension rate across the interior of the Great Basin of the western United States at the latitude of ~39°N. The study area includes faults bounding the Desatoya, Toiyabe, Monitor, Simpson Park, Toquima, Antelope, Fish Creek, Butte, Egan, and Schell Creek Ranges. The rate of earthquake recurrence is documented to be significantly less than observed within the Walker Lane–Central Nevada seismic belt and along the Wasatch, which respectively define the western and eastern boundaries of the interior of the Great Basin. Late Pleistocene extension across the interior of the Great Basin is calculated to equal ~1 mm/yr across the 450 km transect and is consistent with rates defined by recent geodetic studies. The agreement in extension rate estimates over different time scales indicates that tectonic deformation in the Great Basin has been characterized by relatively slow and consistent extension through the late Pleistocene to the present. The internal deformation of the Great Basin and the pattern of strain release may reflect a broad transition zone from northwest-directed shear in the west to extension along the eastern edge of the Pacific–North American plate boundary.

INTRODUCTION

The ~700-km-wide Great Basin encompasses over two thirds of the ~1000-km-wide Pacific–North American plate boundary and is characterized by Basin and Range topography (Fig. 1). Geologic studies and modern space-based geodetic studies indicate that ~50 mm/yr of relative right-lateral deformation is distributed across the boundary (DeMets and Dixon, 1999). The majority of the deformation is localized along the San Andreas fault system in California (Savage et al., 2004; Freymueller et al., 1999). Approximately 15%–25% is distributed east of the Sierra Nevada across the Great Basin (Hammond and Thatcher, 2004, 2007; Bennett et al., 1998, 1999, 2003; Dixon et al., 1995; Minster and Jordan, 1987; Thatcher, 2003; Thatcher et al., 1999; Wernicke et al., 2000). The majority of the motion in the Great Basin is concentrated within the Walker Lane, with a lesser amount of geodetically measured strain observed yet further east within the central and eastern Great Basin and the Wasatch Front (Fig. 1A).

We here characterize the late Pleistocene rates of displacement and paleoseismic history of normal faults bounding ten mountain range fronts distributed across U.S. Highway 50, including the Desatoya, Toiyabe, Toquima, Monitor, Simpson Park, Antelope, Fish Creek, Butte, Egan, and Schell Creek Ranges (Fig. 1B). Information on the timing and amount of strain released by late Pleistocene earthquakes defines the manner in which contemporary strain across the region is ultimately accommodated by brittle deformation. Thus, the long-term geologic record of earthquake displacements and the relative age of faulted deposits are used to estimate a late Pleistocene extension rate. In this paper, we use the regional distribution of paleoearthquakes in time and space to make a first-order comparison of the rate of strain release recorded by faulting with the rate of strain accumulation reported by geodecists elsewhere. We then discuss the pattern of deformation in the context of the width of deformation associated with the Pacific–North American plate boundary.

BACKGROUND (GEOLOGY, GEODESY, EARTHQUAKE GEOLOGY)

Geologic Framework

The Pacific–North American plate boundary in the western United States is characterized by a broad diffuse zone of deformation distributed between the eastern front of the Basin and Range and the western continental shelf (Fig. 1A; Hamilton and Myers, 1966; Atwater, 1970; Minster and Jordan, 1987; Dixon et al., 1995; Bennett et al., 1999). Across present-day Nevada and Utah, the geographical distribution and structural development of mountain ranges reflect temporal changes in the style and rate of faulting from the Mesozoic to the present. Contractional orogenies related to the subduction of the Farallon plate beneath North America during the Mesozoic resulted in a thickening of the continental crust and development of thrust faults in the Basin and Range (Allmendinger, 1992; Coney and Harms, 1984; Dickinson and Snyder, 1979; Livaccari et al., 1981). An overprinting extensional regime was established in the Basin and Range by the late Paleogene and was associated with core complex formation along low-angle detachment faults (Coney, 1987; Armstrong and Ward, 1991; Wernicke, 1992; Coney and Harms, 1984; Bartley et al., 1988; Taylor et al., 1989; Gans et al., 1989; Humphreys, 1995; Sonder and Jones, 1999). From Miocene to present time, extensional deformation within the Great Basin has been influenced by plate-boundary forces related to growth of the San Andreas fault system and buoyancy forces internal to the crust and lithospheric mantle (Sonder and Jones, 1999; Atwater, 1970). High-angle normal faulting (block faulting) along predominantly north- and northeast-trending mountain ranges is the primary process controlling the modern physiographic expression of evenly spaced mountains and valleys in the Great Basin (Fig. 1B; Wallace 1984a, 1984b; Stewart, 1971,

[†]E-mail: rich.koehler@alaska.gov

GSA Bulletin; March/April 2011; v. 123; no. 3/4; p. 631–650; doi: 10.1130/B30111.1; 9 figures; 4 tables; Data Repository item 2011012.

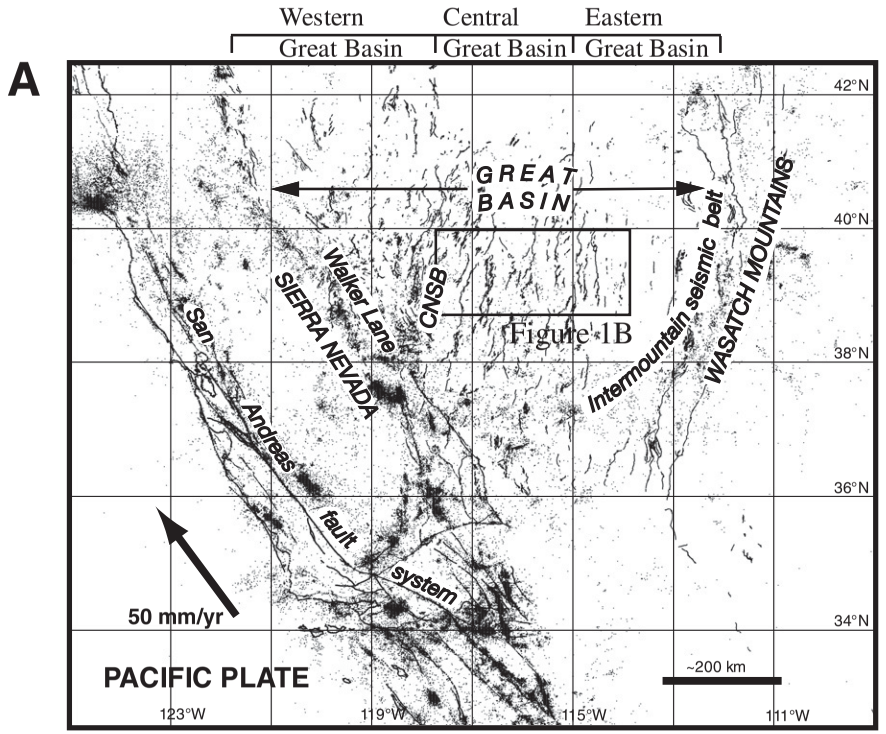

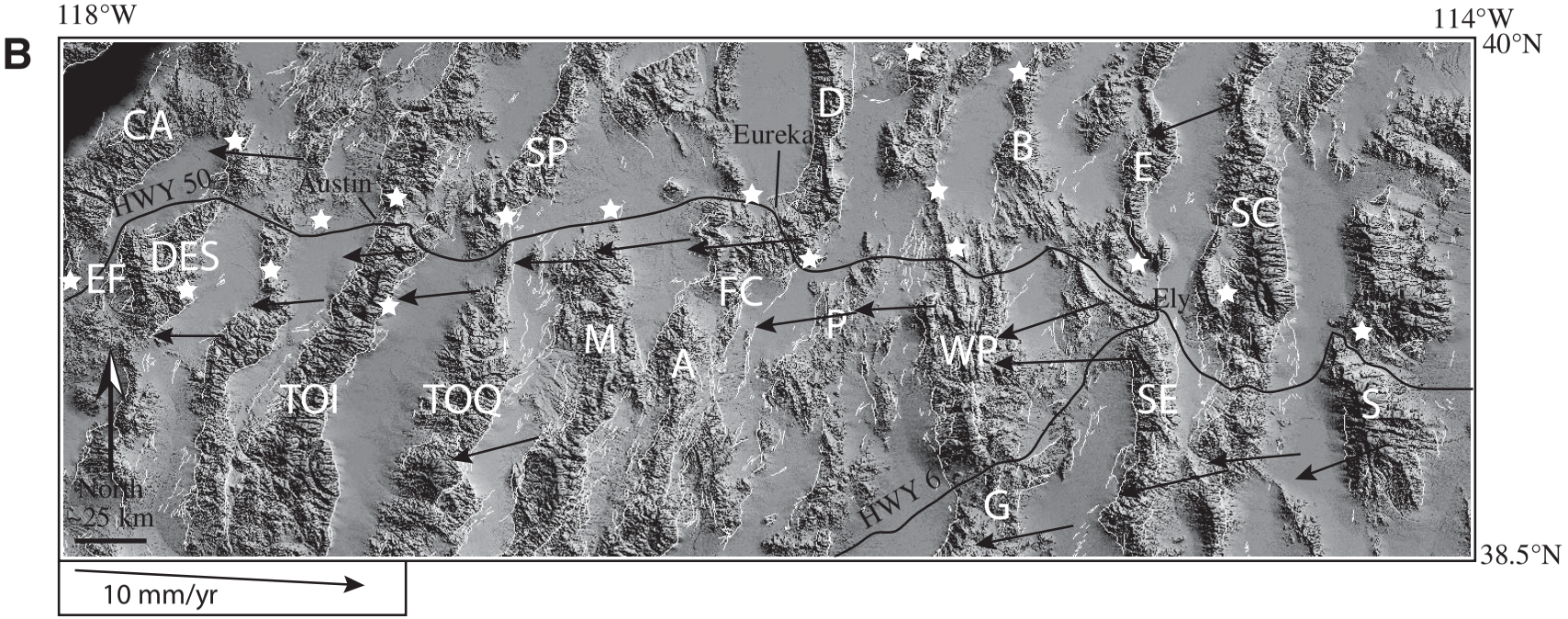

Figure 1. (A) Active faults and seismicity of the Pacific–North American plate boundary in western United States. Faults are shown by black lines, and seismicity is shown by black dots; major tectonic elements of the Great Basin are also labeled. Seismicity is M > 2 (since 1944) from Advanced National Seismic System's catalog (http://quake.geo.berkeley.edu/anss/catalog-search.html). Faults are from Dohernwend et al. (1996) and the Fault and Fold Database of the U.S. Geological Survey (Haller et al., 2004: http://qfaults.cr.usgs.gov). Plate motion velocity vector is from DeMets and Dixon (1999). Approximate boundaries of provinces within the Great Basin were taken from Bennett et al. (2003). (B) Location of normal fault–bounded mountain ranges within the Great Basin that are the focus of this study. Also indicated are mountain ranges referred to in the text. Faults were taken from the Fault and Fold Database of the U.S. Geological Survey (Haller et al., 2004: http://qfaults.cr.usgs.gov). White stars are permanent global positioning system (GPS) monuments recently installed as part of the EarthScope element of the Plate Boundary Observatory project. Black arrows are crustal velocity vectors modified from Hammond and Thatcher (2004). U.S. Highway 50 and Highway 6 are shown in black. EF—East Gate fault; CA—Clan Alpine Range; DES—Desatoya Range; TOI—Toiyabe Range; TOQ—Toquima Range; SP—Simpson Park Mountains; M—Monitor Range; A—Antelope Range; FC—Fish Creek Range; D—Diamond Range; P—Pancake Range; WP—White Pine Range; G—Grant Range; B—Butte Range; E—Egan Range; SE—South Egan Range; SC—Schell Creek Range; S—Snake Range.

1978; Gilbert, 1928). The structure is attributed to narrow zones of extension related to fragmentation of a brittle crust over a plastically extending substratum (Stewart, 1971). When combined with earlier low-angle detachment faulting, the aggregate amount of extension comes to around 150 km (Wernicke, 1992; Coogan and DeCelles, 1996).

The physiographic expression of ranges across the region changes from north-south–oriented ranges bounded by normal faults in the eastern Great Basin to progressively more northeast-oriented ranges within the central Great Basin, where range-front normal faults commonly diverge from the range front and extend into valleys in left-stepping en echelon patterns. Northeast-trending ranges abruptly terminate against northwest-trending ranges along the eastern side of the Central Walker Lane (Fig. 1A). This abrupt boundary defines an overlapping transition between Basin and Range–style extensional deformation to the north and east and transform deformation related to Pacific–North American relative plate motion to the southwest.

Geodetic Background

First-order spatial and temporal patterns of strain accumulation across the western United States have now been defined by geodesy (Minster and Jordan, 1987; Argus and Gordon, 1991; Dixon et al., 1995, 2000; Hammond and Thatcher, 2004, 2007; Bennett et al., 1998, 1999, 2003; Thatcher et al., 1999; Thatcher, 2003; Wernicke et al., 2000; Savage et al., 1995; Svarc et al., 2002b). Deformation in the Walker Lane is characterized by ~10 mm/yr of right-lateral shear parallel to the San Andreas fault system. Deformation to the east from the Central Nevada seismic belt to the Wasatch is dominated by easterly extension. Geodesy limits east-west extension rates to <~3 mm/yr between the Central Nevada seismic belt and Intermountain seismic belt (Wernicke et al., 2000; Bennett et al., 1998, 2003; Hammond and Thatcher, 2007), and the majority of that (~1.6 mm/yr) is focused along the Wasatch fault zone (Chang et al., 2006). Geodetic moment accumulation is closely correlated to seismic moment release rates across the Great Basin (Pancha et al., 2006).

Earthquake Geology

Paleoseismic investigations throughout the Great Basin, including the Walker Lane, Central Nevada seismic belt, and Intermountain seismic belt, have begun to elucidate long-term spatial and temporal patterns of earthquake recurrence, particularly along the basin margins. A summary of the paleoseismic histories reported in those studies is provided in Table 1. We defer discussion of those results until later in the Discussion section, where they are used to provide context for interpretation of the results we report here within the interior of the basin.

METHODS

Fault Trenching

Structural, stratigraphic, and pedogenic relations exposed in natural exposures or trenches excavated normal to fault traces are the basis to place bounds on the paleoseismic history of faults at eight sites within the study area. The approach is described in McCalpin (1996). Detailed stratigraphic unit descriptions for each trench are archived in Koehler (2009) and summarized in the GSA Data Repository (Electronic Supplement 1).[1]

Scarp Profile Analysis

Fault scarp profiles were surveyed with a total station or by differential global positioning system (GPS) to obtain measurements of vertical displacement along each of the fault scarps investigated. The profile data were also used in diffusion analyses of fault scarp morphology to estimate the age of the earthquakes that produced the scarps, under the assumption that the initial scarp was produced by a single earthquake (Bucknam and Anderson, 1979b; Wallace, 1977; Hanks and Wallace, 1985). The diffusion equation for scarps in Quaternary alluvium is

$$du/dt - \kappa(d^2u/dx^2) = 0, \quad (1)$$

where u is the relative elevation of a point on the scarp, which is a function, $u(x,t)$, of the horizontal distance perpendicular to the scarp (x) and time (t), and κ is a diffusivity constant with units of m^2/k.y. (Hanks, 2000; Hanks and Wallace, 1985). For faulted Quaternary deposits, where the initial slope is not flat, the solution to the diffusion equation is a function of the hanging-wall and footwall slopes, the initial offset, κt, and an assumed value of friction (μ) that defines the initial angle of repose for a scarp in weakly consolidated materials (Hanks and Andrews, 1989). We generated synthetic profiles for specific values of time, keeping the slope and offset constant, to determine the best fit to the observed profile. The results provided an estimate for the age of the earthquake that created the respective scarp.

Diffusion modeling of fault scarps is considered a reconnaissance tool with inherent uncertainties, outlined in Hanks (2000). The primary uncertainties include determination of κt, the κ value used to reduce that κt to an age estimate, and the applicability of κ to the scarp of interest. A multitude of factors can cause κ to vary, including lithology, carbonate accumulation, rainfall, and vegetation, among others. This uncertainty can be reduced by using a value of κ consistent with values determined in a similar environment. For the Basin and Range, values of κ previously determined in diffusion studies of independently dated fault scarps in loosely consolidated alluvium and shoreline scarps of Lake Lahontan and Lake Bonneville range between ~0.9 and 1.2 m^2/k.y. (Hanks, 2000; Hanks et al., 1984; Hanks and Wallace, 1985). We used values of friction (μ = 0.75) and mass diffusivity (κ = 1 m^2/k.y.) that are consistent with those studies, as well as those used in recent paleoseismic studies in the Great Basin that had independent age control (Wesnousky et al., 2005). The age of deposits from which the bulk of κ estimates come from is generally <15 k.y., and, thus, the fault scarp modeling technique is best applied to latest Pleistocene to Holocene fault scarps. The root mean squares of the uncertainty in κt and κ for youthful scarps in the Basin and Range yield values ~70% about the age of the scarp (Hanks, 2000). It is not well understood how stable the value of κ is farther back in time, and thus the error in the age estimation of late Pleistocene scarps in this study is inferred to be ±10–15 k.y. To reduce uncertainty, we modeled scarps of similar size to those used to determine κ elsewhere in the Basin and Range. Our estimates of scarp age are exclusive of the epistemic uncertainty of applying values of κ determined elsewhere to fault scarps in this study. We used subsurface exposures and surficial observations to limit our analyses to fault scarps determined to be related to a single event. In cases where subsurface exposures were not available, we assumed a single-event origin for scarps that were small (<~1 m), had smooth profiles devoid of slope inflections, and separated hanging-wall and footwall surfaces characterized by similar morphology.

Additional uncertainties include the amount of time it takes for the scarp-free face to reach the angle of repose and the estimate of the initial offset. Inspection of scarps produced in historic

[1]GSA Data Repository item 2011012, Electronic Supplement 1, stratigraphic descriptions from trenches; Electronic Supplement 2, fault scarp profiles and diffusion analyses; Electronic Supplement 3, location maps, surficial geologic strip maps, and other supporting information, is available at http://www.geosociety.org/pubs/ft2010.htm or by request to editing@geosociety.org.

TABLE 1. PALEOSEISMIC SUMMARY FOR FAULTS IN NEVADA AND UTAH BETWEEN 38.5°N AND 40°N LATITUDE

Fault*	Number and timing of events†, and slip rate	Reference§
2. Peavine Peak	4–5 events in last 6000–8000 yr	a
4. Warm Springs	At least 3 events in latest Pleistocene	E
5. Pyramid Lake	at least 4 events post–ca. 15,500 cal yr B.P.; MRE after 1705 ± 175 cal yr B.P.	c
1. Genoa	2 events, 500–600 cal yr B.P.; 2000–2200 cal yr B.P.	b
D. 1954 Rainbow-Stillwater	3 events: 1954 AD; 6.3–9.9 ka; 8.1–17.8 ka; plus event at 0.0–1.5 ka on Fourmile Flat strand. Slip rate 0.4 mm/yr; post–latest Pleistocene slip rate 0.2–0.46 mm/yr	de
C. 1954 Dixie Valley	3 events: 1954 AD; 2.0–2.5 ka; <35 ka	fe
B. 1954 Fairview Peak	2 events: 1954 AD; >35 ka	ge
A. 1932 Cedar Mt.	6 events: 1932 AD; 4 ± 2 ka; 5 ± 2 ka; 12 ± 2 ka; 15 ± 2 ka; 18 ± 2 ka	h
14. Desatoya (W)	3 late Pleistocene events#; MRE latest Pleistocene <20 ka? ± 10#,**	i
15. Desatoya (E)	At least 1 late Pleistocene event, predates highstand of Lake Desatoya	i
12. Eastgate	3 events in last 28 ka, MRE before 4.4 ka; penultimate ca. 17 ka	G
13. Clan Alpine	2 or 3 events post–ca. 130 ka; MRE before 9 ± 1 ka; penultimate before 28 ± 3 ka	j
16. Toiyabe (W)	At least 2 late Pleistocene events based on beveled 4-m-high scarp	i
18. Toiyabe (E)	2 events in late Pleistocene#,**, MRE latest Pleistocene	i
23. Toquima	Southern part, at least 1 event: ca. 55–60 ka††, Northern part (Hickison Summit area), at least 1 event ca. 16 ka††	i
22. Simpson Park	2 events: MRE 6–9 ka†† and post–ca. 15,500 cal yr B.P.; penultimate pre–Lake Gilbert highstand	i
24. Monitor (W)	1 event: ca. 44 ka††	i
Monitor (E)	At least 1 late Pleistocene event	i
25. Antelope	2 events: ca. 15–21 ka††; ca. 44–66 ka††	i
26. Fish Creek	1 event: ca. 28–29.7 ka††	i
27. Diamond Range (E)	At least 1 late Pleistocene event, predates highstand of Lake Newark	i, F
28. Butte	3 late Pleistocene events: MRE ca. 18–25 ka††,**; 2 older events	i
31. Egan (E)	1–2 events: ca. 21–36 (?) ka††; ca. 60 ka††,**	i
32. Schell Creek	2–3 late Pleistocene events: 1–2 events between ca. 10 and 30 ka††,** and 1 older event	i
33. Snake Valley	At least 1 event <15 ka, 2.4 m displacement	oH
34. Deep Creek Range (E)	At least 1 event, middle to late Pleistocene, scarps ~13 m	oH
36. House Range	At least 1 event: ca. 12–19 ka and post-Bonneville transgression	lm
35. Fish Springs	4 events post-Bonneville highstand: MRE ca. 2 ^{14}C ka–4.8 ka††	nopqr
37. Crickett Mt.	At least 2 events: MRE post-Provo shoreline; penultimate pre-Bonneville	sto
38. Drum Mt.	At least 2 events: MRE between ca. 12 ka†† and early Holocene; penultimate pre-Bonneville	ouvwqx
39. Clear Lake	1 event: Holocene	vt
44. Little/Scipio V.	Red Canyon scarps: surface displacement of 2.2 m in latest Pleistocene to Holocene; Maple Grove fault: cumulative displacement of 12 m, late Pleistocene predating Bonneville highstand; Pavant Range fault: at least 1 Holocene event; Scipio Valley fault: cumulative late Pleistocene displacement of 11 m and 1 late Holocene event with 2.7 m displacement; Little Valley fault, cumulative displacement of 8.2 m, late Pleistocene predating Bonneville highstand.	ovy
45. Japanese V.	At least 1 event, offset 4 m, late Pleistocene to Holocene	tz
47. Southern Wasatch	Nephi segment; MRE after 1350 ± 70 ^{14}C yr B.P., penultimate before 3841 cal yr B.P.; oldest after 5300 ± 300 ka. Levan segment: 2 events: MRE after ca. 2 ka multiple dates; penultimate before 3.1 ka. Fayette segment: at least 1 event ca. 10–15 ka†	ABCD

Note: Fault numbers correlate to faults on Figure 9. Information for faults shown on Figure 9 that are north of 40°N latitude is contained in Wesnousky et al. (2005) and Koehler (2009).

*(W) or (E) indicates west or east side of range. Southern Wasatch includes Nephi, Levan, and Fayette segments.

†Surface rupture. Uncorrected ages in thousands of years are listed as ka; calibrated radiocarbon ages are listed as cal yr B.P.; MRE—most recent earthquake.

§References: a—Ramelli et al. (2004); b— Ramelli et al. (1999); c—Briggs and Wesnousky (2004); d—Caskey et al. (2004); e—Bell et al. (2004); f—Bell and Katzer (1990); g—Caskey et al. (2000); h—Bell et al. (1999); i—this study; j—Machette et al. (2005); k—Friedrich et al. (2004); l—Piekarski (1980); m—Sack (1990); n—Machette (1990); o—Hecker (1993); p—Bucknam et al. (1989); q—Hanks et al. (1984); r—Sterr (1985); s—Anderson and Bucknam (1979); t—Oviatt (1989); u—Crone (1983); v—Bucknam and Anderson (1979a, 1979b); w—Colman and Watson (1983); x—Pierce and Colman (1986); y—Oviatt (1992); z—Witkind et al. (1987); A—Jackson (1991); B—Schwartz et al. (1983); C—Schwartz and Coppersmith (1984); D—Machette et al. (1992); E—dePolo and Ramelli (2003); F—Redwine (2003); G—Crone et al. (2006); H—Schell (1981).

#Observations from trench and soils.

**Based on carbonate development in offset fan.

††Best estimate from fault scarp profiling. Uncertainty is ~10 k.y.

ruptures in Nevada indicated that it takes on the order of several hundred years for scarps to reach the angle of repose, and thus age estimates are generally underestimated by that amount. Deposition on the hanging wall after a scarp was created can result in an underestimation of the initial offset and result in an age older than the true age of the scarp. Based on the assumption that deposition occurs shortly after the scarp is produced, as streams cutting through the scarp adjust to base-level change, we infer that most of the scarp diffusion occurs after the deposition and that the modeled age is little affected.

Examples of diffusion models for relatively old, intermediate, and young fault scarps are

shown in Figure 2, and a compilation of the synthetic and measured scarp profiles used in this study is given in the GSA Data Repository (Electronic Supplement 2 [see footnote 1]). The location of the profiles, estimated age for the earthquakes that created the scarps, and the measured vertical separations are cataloged in Table 2 and were used to estimate the cumulative vertical and horizontal displacement across the transect (shown in Tables 3 and 4).

Dating of Alluvial Surfaces and Subsurface Deposits

Geomorphic markers were used to identify the relative age and extent of earthquake ruptures preserved in Quaternary alluvium across the U.S. Hwy 50 transect. The stratigraphic chronology is based on surficial mapping and geomorphic principles used to differentiate and/or correlate alluvial units, including relative degree of incision and rounding of surface morphology, cross-cutting depositional and inset relations, amount of offset along fault scarps, where progressively older surfaces are preserved at higher elevations, color, texture, and character of incision on air photos, and soil development. Highstand shoreline deposits associated with pluvial lakes provide a late Pleistocene time stratigraphic datum useful for relative age assessment throughout the region (Adams and Wesnousky, 1998; Mifflin and Wheat, 1979; Reheis, 1999).

Soil development, in particular, B-horizon clay and pedogenic carbonate, progressively increases with time (Birkeland, 1999; Machette, 1985a; Jenny, 1941). Thus, we used these parameters to place broad age constraints on displaced surfaces and maximum age estimates for the observed offsets. Soils and carbonate stage development were described based on criteria outlined in Birkeland et al. (1991), Gile et al. (1966), Bachman and Machette (1977), Machette (1985b), and Birkeland (1999). Although clast lithologies, temperature, and precipitation are slightly variable across the Great Basin, we made the simplifying assumption that changes in climate and carbonate available in the environment have been relatively similar across the Hwy 50 transect and soils with similar carbonate stage development have similar relative age. Complete soil descriptions, laboratory clay percent versus depth profiles, and mean annual temperature and precipitation data are archived in Koehler (2009). We draw on observations from previous studies that relate carbonate stage development to independent estimates of deposit age (Machette, 1982, 1985a, 1985b; McFadden, 1982; Harden and Taylor, 1983; Harden et al., 1991, 1985; Reheis, 1987; Treadwell-Steitz and McFadden, 2000; Taylor, 1989; Reheis and Sawyer, 1997; Sawyer, 1990; Slate, 1992; Reheis et al., 1995, 1996; McDonald et al., 2003; Kurth et al., 2010; Redwine, 2003). Combined, these studies indicate that soils that exhibit stage II to II+ carbonate development are late middle Pleistocene to late Pleistocene in age (ca. 50–175 ka) (Redwine et al., 2010, personal commun.).

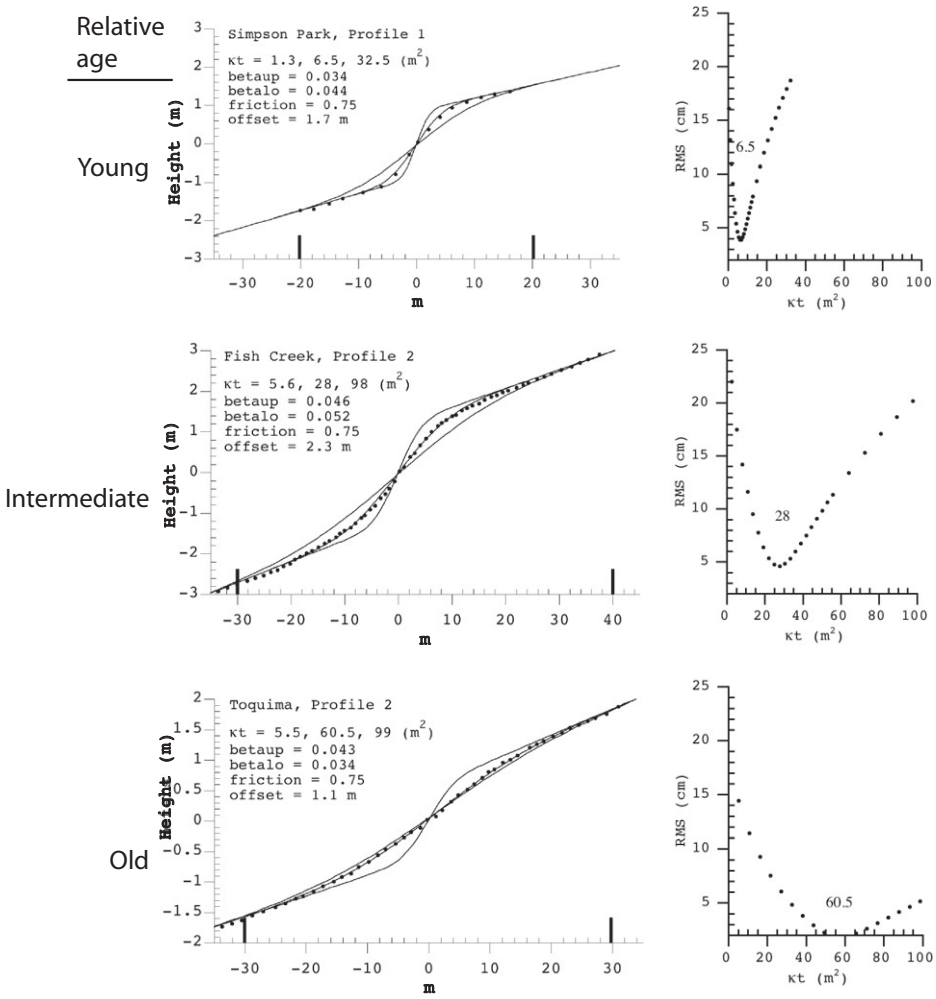

Figure 2. Examples of the approach used to estimate the age of single-event fault scarps based on surveyed scarp profiles and diffusion analyses. Examples are shown for scarps of relatively young, intermediate, and old age. Plots of the root mean square (RMS) misfit between observed and synthetic profiles versus a range of κt indicating closeness of fit is shown to the right of each profile. In total, 32 scarp profiles were used in the analysis and are archived in Electronic Supplement 2 (see text footnote 1). Profiles from multiple event scarps were used only to estimate vertical separation.

The ages of subsurface deposits that constrain the timing of earthquakes were determined based on tephra correlation (Sarna-Wojcicki and Davis, 1991), correlation with pluvial lake highstand deposits, and relative degree of soil development in strata buried by fault scarp colluvium (Birkeland, 1999). The lack of preservation of organic material in the arid alluvial deposits of the study area limited the utility of radiocarbon dating. The results of the tephrochronology, radiocarbon, and bulk soil sieve analyses are recorded in Koehler (2009).

Surficial Geologic Mapping

Aerial reconnaissance of the study region was performed to identify surficial geologic map units and fault traces using (1) LandSat images, digital orthophotoquads (DOQs), and digital elevation models (DEMs), (2) 1:60,000 scale black and white aerial photographs, (3) 1:10,000 scale low-sun-angle black and white air photos, and (4) existing maps of fault traces and Quaternary deposits (Dohernwend et al., 1992, 1996; Haller et al., 2004; Schell, 1981). Field mapping was

TABLE 2. VERTICAL SEPARATION MEASURED FROM FAULT SCARP PROFILES AND BEST ESTIMATE OF SCARP AGE BASED ON DIFFUSION ANALYSIS

Range	Profile name	Easting	Northing	Vertical displacement (m)	Estimate of scarp age (ka)
Desatoya	Profile 1	436060.5625	4370546.5	2.3	N.A.
	Profile 2	436079.03125	4370557.0	2.5	N.A.
Toiyabe	Profile 1	498115.5	4353974.77	1.8	N.A.
Simpson Park	Profile 1	536419.4131	4421281.38	1.7	6.5
	Profile 2	535605.25	4410974.0	4.2	9
Toquima	Profile 1	515296.0625	4300354.0	1.87	55
	Profile 2	525610.4375	4320799.5	1.1	60
	Profile 3	526196.375	4374000.0	1.1	16
Monitor	Profile 1	532403.75	4350846.0	0.85	44
	Profile 2	532385.5	4350775.0	0.85	44
Antelope	Profile 1	561383.125	4338642.5	3.7	N.A.
	Profile 2	562414.625	4340731.5	3.0	N.A.
	Profile 3	570345.313	4354190.5	1.7	21
	Profile 4	570330.1875	4354168.5	1.6	15
Fish Creek	Profile 1	580752.8125	4346358.0	2.7	29.7
	Profile 2	580736.3125	4346351.0	2.3	28
Butte	Profile 1	645689.5	4403714.5	0.95	18
	Profile 2	645691.375	4403705.0	1.3	22
	Profile 3*	643470.4856	4399653.5	4.2	22
	Profile 4*	643470.4856	4399653.5	4.4	25
	Profile 5	642651.875	4397001.5	5.3	N.A.
Egan	Profile 1	686397.875	4394087.5	1.3	42
	Profile 2	686394.4375	4394098.5	1.3	60
	Profile 3	681015.4375	4383295.0	2.2	N.A.
	Profile 4	681010.1875	4383286.5	1.6	N.A.
Schell Creek	Profile 1	713815.875	4343132.0	1.04	N.A.
	Profile 2	713815.75	4343135.5	0.98	N.A.
	Profile 3	713450.875	4343035.0	0.84	N.A.
	Profile 4	713447.25	4343040.0	0.77	N.A.
	Profile 5	711908.625	4374068.0	3.85	30
	Profile 6	711912.75	4374018.0	3.7	35
	Profile 7	711917.75	4373988.0	3.6	32

Note: Diffusion analyses assume following values of friction ($\mu = 0.75$) and mass diffusivity ($\kappa = 1$ m^2/k.y.). Age estimates are not provided for scarps that are not characterized by matching hanging-wall and footwall surfaces or were determined to be related to multiple events. Coordinates for each profile are in WGS84 projection.

*Coordinates for profiles 3 and 4 along the Butte Range are actually the coordinates of the trench. The profiles were surveyed ~4 m north and south of the trench.

focused in areas most likely to preserve a record of fault displacements in late Quaternary deposits of various ages. Interpretation of geomorphic surfaces and the extent of fault scarps were field verified along each range and compiled on 1:24,000 scale 7.5′ U.S. Geological Survey topographic quadrangles. Geologic map units identified across the region are depicted schematically in Figure 3. Detailed descriptions of sedimentological properties and air photo characteristics of each map unit are contained in Koehler (2009) and generalized next. Figure 4 shows an aerial photograph of the northern Simpson Park Mountains area that is representative of the Quaternary geologic units observed throughout the study region. The surficial geologic maps for each range studied, encompassing a total distance of >300 km, are contained in Electronic Supplement 3 (see footnote 1).

Quaternary Stratigraphy

Very old alluvial-fan deposits and pediment surfaces (QTp) occur in isolated areas along some range fronts. QTp surfaces have similar surficial characteristics to old alluvial-fan surfaces (Qfo), with the exception of greater amounts of incision and rounding between stream interfluves. Active fault traces extend across the base of QTp surfaces and are responsible for their position and preservation. No exposures of soils developed into QTp surfaces were observed; however, based on their topographic position above Qfo deposits and geomorphic antiquity, QTp surfaces may have been abandoned in the early Pleistocene or Pliocene.

Old alluvial-fan deposits (Qfo) occur as small, irregularly shaped landforms along range fronts where the active fault steps across the piedmont slope. Large coalesced (Qfo) fan complexes that extend up to several kilometers into valleys are associated with range fronts characterized by either long recurrence intervals or absence of active faulting. Isolated, back-tilted Qfo remnants also occur along fault traces and grabens in midvalley areas. Qfo surfaces are characterized by smooth, rounded morphology between drainages, well-developed dendritic drainage pattern, and deep incision (5–25+ m). Based on thick carbonate coatings on bioturbated clasts, multiple buried Btk horizons with stage III+ to IV carbonate stage development (Birkeland, 1999), and topographic position above intermediate-aged alluvial-fan surfaces (Qfi), we infer that Qfo surfaces are middle Pleistocene or older in age.

Intermediate alluvial fans (Qfi) exist along range fronts and also emanate from channels cut into remnant alluvial deposits (Qfo). Qfi surfaces are inset 1–5 m into older alluvial surfaces and have been incised between 2 and 4 m by ephemeral streams. Lacustrine constructional features are deposited on Qfi surfaces and mimic the conical topographic shape of the underlying Qfi fan. Qfi surfaces are characterized by broad, flat relatively undissected morphology between stream channels, and a weak dendritic drainage pattern. Qfi deposits have moderately thick carbonate coatings on bioturbated clasts on the surface and moderately thick Bk soil horizons (20–40 cm) that have stage II to II+ carbonate stage development (Birkeland, 1999). Qfi surfaces are buried by and predate Lahontan age (latest Pleistocene) deposits. Based on comparison to carbonate morphology developed in other soils in the region, Qfi deposits may have been deposited between 50 and 175 ka. This age range is consistent with ^{10}Be surface exposure ages

TABLE 3. EARTHQUAKE DISPLACEMENTS FOR LAST ~60 k.y.

Fault*	Vertical separation† (m)	Extension (m)	Strike (°)	HEW (m)
13. Clan Alpine (E)	6[t]	3.5	27	3.1
12. Eastgate (W)	6.9[t]	4	327	3.3
14. Desatoya (W)	2.5[p]	1.4	50	0.9
15. Desatoya (E)	6[f]	3.5	32	2.9
23. Toquima North (Hickison Summit) (E)	1.1[p]	0.6	35	0.5
22. Simpson Park (W)	4.2[p]	2.4	35	2.0
16. Toiyabe (E)§	3.3[pf]	1.9	32	1.6
18. Toiyabe (W)	4.0[f]	2.3	29	2.0
23. Toquima South (E)	3.0[p]	1.1	32	0.9
48. Monitor (E)	2[f]	1.2	45	0.8
24. Monitor (W)#	1.7[pf]	1.0	15	0.9
25. Antelope (W)	3.7[p]	2.1	27	1.9
26. Fish Creek (E)	2.7[p]	1.6	15	1.5
27. Diamond (E)	3[f]	2.3	0	2.3
28. Butte (W)	5.3[p]	3.1	10	3.0
31. Egan (E)	2.2[p]	1.3	15	1.2
32. Schell Creek (E)	3.85[p]	2.3	0	2.3
33. Snake Valley (E)	2.4	1.4	0	1.4
34. Deep Creek (E)	?	?	20	?
35. Fish Springs (E)	3.3[p]	1.9	358	1.9
36. House (W)	1.4[f]	0.8	0	0.8
37. Crickett Mts. (W)	1.3[f]	0.8	17	0.7
38. Drum Mts. (E)	2.4[ft]	1.4	353	1.4
39. Clear Lake (E)	3[f]	1.7	351	1.7
44. Little/Scipio Valley (E)	12[f]	6.9	0	6.9
45. Japanese/Cal Valley (W)	4[f]	2.3	4	2.3
SUM	91.3	58.5		48.4
			Extension rate = 48.4 m/60 k.y. = 0.8 mm/yr	

Note: Estimate does not include range fronts with prominent tectonic geomorphology where alluvial surfaces are not offset. Fault numbers correlate to faults on Figure 9. HEW—Horizontal east-west extension.

*Fault dip direction indicated by E (east) and W (west). Fault number corresponds to faults on Figure 9.

†Method used to estimate vertical separation. t—interpreted from trench exposure; p—scarp profile; f—field measurement with hand level or previously reported height from field mapping studies. References for each fault are the same as those reported in Table 1.

§Scarp profile measurement combined with hand-level scarp height of secondary scarp to estimate total separation.

#Total separation estimated by combining scarp profile measurement and height of a similar scarp upslope.

(ca. 50–105 ka) determined for alluvial fans in the Death Valley area that have similar surficial characteristics and soils to the surfaces in our study (Frankel et al., 2007a, 2007b). The similarity of clay percent profiles (Koehler, 2009) and carbonate development in soils developed in Qfi surfaces across the region suggests relatively synchronous deposition. The apparent sychroneity of Qfi deposits may be related to regional aggradation, suggested by Eppes et al. (2003) to have occurred during climatic transitions between oxygen isotope stage (OIS) 4–OIS 3 (ca. 70 ka) and OIS 6–OIS 5 (ca. 130 ka); however, the OIS 4–OIS 3 transition may be as young as 57 ka (Lisiecki and Raymo, 2005).

Young alluvial-fan deposits (Qfy) include active wash and alluvial-fan deposits that are inset into pre–latest Pleistocene alluvial surfaces. These surfaces originate in channels at the mountain front or within channels at the outboard edge of older elevated alluvial surfaces. Qfy surfaces are deposited on and inset into Qfi surfaces in downslope and upslope areas, respectively. Qfy deposits commonly extend to the valley floor and cut pluvial lake deposits. Small Qfy surfaces bury fault traces and older alluvial-fan deposits along some range fronts. Qfy surfaces are characterized by fresh bar and swale morphology, conical shapes with a well-defined crest, and broad distributary drainage networks. Youthful morphology, weak soils that have stage I carbonate stage development (Birkeland, 1999), and crosscutting relations with pluvial lake deposits indicate that Qfy surfaces are latest Pleistocene to Holocene in age and generally postdate Lahontan-age (latest Pleistocene) lake landforms.

Basin-fill deposits (Qbf) represent a composite of deposits, including those related to distal fan, pluvial lake, ephemeral stream, and eolian processes. Quaternary to Holocene playa deposits (Hp) and lacustrine deposits (Ql) occur in the middle of basins, onlap pre–latest Pleistocene alluvial-fan deposits at basin margins, and occur locally as playettes, i.e., flat areas behind highstand constructional deposits. Holocene dune deposits (Hd) form narrow discontinuous bands of loose sand and silt that fringe the edges of some basins. Latest Pleistocene alluvial-fan deposits have incised and buried lacustrine deposits in upslope and downslope areas, respectively. Lacustrine beach deposits Qbb of paleolakes form broad, flat, curvilinear bands with convex-up cross-sectional morphology in map view. Well-preserved constructional landforms typically have thin, weakly developed soils similar to soils developed in latest Pleistocene deposits of the Sehoo highstand of pluvial Lake Lahontan (Adams and Wesnousky, 1999).

Across the region, each map unit exhibits similar sedimentologic, morphologic, and pedologic characteristics. These similarities may reflect regional climatic patterns that caused alternating periods of alluvial-fan and pluvial lake development and periods of relative incision and downcutting. Although temporally and spatially synchronous geomorphic processes may have occurred across the transect, determination of the exact age of individual surfaces mapped as similar age (e.g., Qfi) is problematic and may vary by several tens of thousands of years or more. Given these uncertainties, the regional stratigraphic framework is consistent throughout the study region and provides a means to compare relative rates of tectonic activity.

Calculation of Extension Rate

Observed late Pleistocene vertical displacements were converted to horizontal displacements along each fault based on assumptions attendant to the dip of the fault and the geometrical relations shown in Figure 5. We assumed a 60° dip for the faults at seismogenic depths

TABLE 4. EARTHQUAKE DISPLACEMENTS FOR LAST ~20 K.Y.

Fault*	Vertical separation† (m)	Extension (m)	Strike (°)	HEW (m)
13. Clan Alpine (E)	1.2[t]	0.7	27	0.6
12. Eastgate (W)	1[t]	0.6	327	0.5
14. Desatoya (W)	0.8[t]	0.5	50	0.3
23. Toquima North (Hickison Summit) (E)	1.1[p]	0.6	35	0.5
22. Simpson Park (W)	4.2[p]	2.4	35	2.0
18. Toiyabe (E)	0.4[t]	0.2	32	0.2
25. Antelope (W)	1.7[p]	1.0	27	0.9
28. Butte (W)	1.3[p]	0.8	10	0.7
32. Schell Creek (E)	1.9[p]	1.4	0	1.4
33. Snake Valley (E)	2.4	1.4	5	1.4
35. Fish Springs (E)	3.3[p]	1.9	358	1.9
36. House (W)	1.4[f]	0.8	0	0.8
37. Crickett Mts. (W)	1.3[f]	0.8	17	0.7
38. Drum Mts. (E)	3.7[tt]	2.1	353	2.1
39. Clear Lake (E)	3[f]	1.7	351	1.7
44. Little/Scipio Valley (E)	2.7[f]	1.6	0	1.6
45. Japanese/Cal Valley (W)	4[f]	2.3	4	2.3
SUM	35.4	24.5		19.3
				Extension rate = 19.3 m/20 k.y. = 1.0 mm/yr

Note: Estimate does not include range fronts with prominent tectonic geomorphology where alluvial surfaces are not offset. Fault numbers correlate to faults on Figure 9. HEW—Horizontal east-west extension.

*Fault dip direction indicated by E (east) and W (west). Fault number corresponds to faults on Figure 9.

†Method used to estimate vertical separation. t—interpreted from trench exposure; p—scarp profile; f—field measurement with hand level or previously reported height from field mapping studies; w—thickness of colluvial wedge. References for each fault are the same as those reported in Table 1.

in accordance with steep dips instrumentally recorded for historic earthquakes in the Great Basin (Doser, 1985, 1986) and frictional constraints associated with Andersonian mechanics (Anderson, 1951). A net cumulative long-term extension rate across the ~500 km transect was estimated by summing the horizontal offsets and dividing by the time period over which the offsets occurred. Displacements along the Wasatch fault, Walker Lane, and Central Nevada seismic belt were omitted from the calculations to isolate deformation internal to the central Great Basin.

OBSERVATIONS

Observations bearing on general faulting characteristics along each range front across the transect are described in detail in Koehler (2009). Electronic Supplement 3 (see footnote 1) contains summary information and supporting figures for each range that show (1) the physiographic expression of the range, extent of previously mapped faults, prominent landmarks, and limits of map areas; and (2) field-based surficial geologic maps depicting fault geometry and distribution of surficial geologic map units, as well as the locations of trenches and scarp profiles. Here, we focus on observations from site-specific paleoseismic field studies that provide information used to interpret the earthquake history, timing, style, and amount of Quaternary displacement along each range. The sum of observations is later used to estimate a long-term extension rate and examine regional deformation patterns.

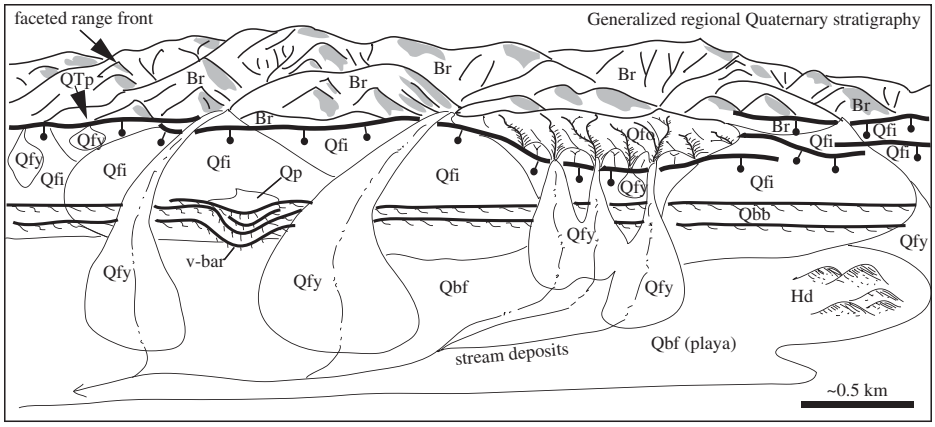

Figure 3. Generalized stratigraphic framework for Quaternary units distributed across the U.S. Highway 50 transect. Stratigraphic units include: Br—bedrock; QTp—Quaternary Tertiary pediment; Qfo—relatively old Quaternary alluvial-fan deposits (middle Pleistocene); Qfi—intermediate-aged alluvial-fan deposits (late Pleistocene); Qfy—relatively young Quaternary alluvial-fan deposits (latest Pleistocene); Qbf—Quaternary basin-fill deposits. Holocene basin-fill deposits include: Qp—playa deposits; Ql—lacustrine deposits; Qbb—shoreline or beach deposits; Hd—dune deposits. Same unit abbreviations are used in Quaternary strip maps and text. On Quaternary strip maps (Electronic Supplement 3 [see text footnote 1]), thick black lines are faults, and blue dashed lines are shoreline features.

Desatoya Range

The northwestern Desatoya range front in the vicinity of Edwards Creek is characterized by subdued range-front morphology, beveled scarps, overlapping, parallel, and left-stepping fault strands, and progressively greater offsets of older alluvial-fan surfaces (Fig. 1B; Electronic Supplement 3, Figs. ES 3.1 and ES 3.2 [see footnote 1]). Fault scarp heights are between 1.5 and 3 m and ~6 m in intermediate (Qfi) and old (Qfo) alluvial surfaces, respectively. Qfy alluvial surfaces have eroded lacustrine deposits of pluvial Lake Edwards and are not displaced by the fault.

A log of a trench excavated across the fault, ~0.5 km west of the Edwards Creek channel, where it produces a scarp in Qfi alluvium, is shown in Figure 6. The trench exposed offset alluvial gravels and a package of colluvial

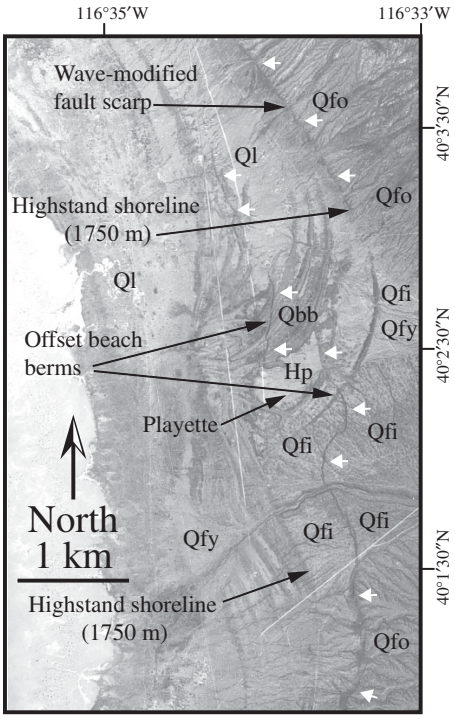

Figure 4. Aerial photograph of the northern Simpson Park Mountains area showing Quaternary geologic units representative of the region. For location of photo, see Electronic Supplement 3, Figure ES 3.8 (see text footnote 1). White arrows denote the location of the Simpson Park Mountains fault. Qfo—relatively old alluvial fan; Qfi—intermediate alluvial fan; Qfy—young alluvial fan; Ql—lacustrine deposits; Qbb—pluvial lake beach berms; Hp—playette deposit. The fault scarp has been modified by wave processes in the northeastern corner of the photo. To the south, the fault displaces a Qfi deposit across an ~1.5 m scarp, and has elevated a Qfo surface >10 m. Note offset recessional shorelines and beach berms associated with pluvial Lake Gilbert that indicate a latest Pleistocene age for the most recent earthquake.

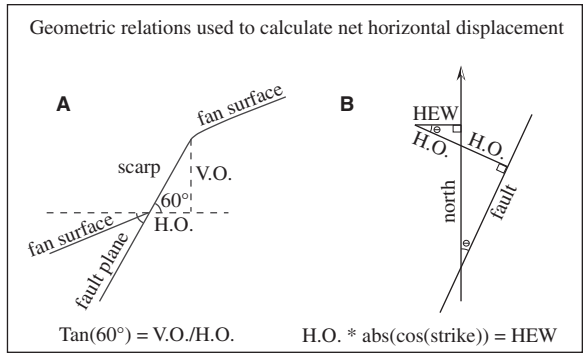

Figure 5. Geometric relations used to calculate net horizontal displacement. (A) Diagram shows an alluvial-fan surface offset across a fault. V.O.—vertical offset obtained from scarp profiles surveyed in the field; H.O.—horizontal offset. Horizontal offset (extension) was calculated assuming a 60° dip for the fault and the geometric relation tan(60°) = V.O./H.O. (B) To obtain a common east-west azimuth for each fault, the calculated extension was multiplied by the abs(cos[strike]) measured clockwise from north and recorded as HEW (horizontal east-west extension) in Tables 3 and 4. The extension along each fault was summed across the transect to estimate the total extension across the Great Basin.

deposits. The stratigraphy is interpreted to record three earthquakes along the western Desatoya Range fault. Unit 3 is fault scarp colluvium that accumulated against the scarp after unit 1 was displaced and back tilted toward the fault by the first (oldest) earthquake. The colluvium (Unit 3) was exposed at the surface long enough for strong clay structure and carbonate nodules to develop. The penultimate earthquake is recorded by unit 4, a colluvium deposited against the fault zone that buries unit 3 and tapers away from the fault. The presence of Bt soil characteristics in the top of unit 4 indicates exposure at the surface prior to burial by unit 5. The separation of units 3 and 4 from unit 1 across an ~1.5-m-wide shear zone (unit 2) characterized by vertically aligned clasts and the deposition of fault scarp colluvium across the fault zone (unit 7) provide evidence for the most recent earthquake. The observations are consistent with surficial evidence for multiple earthquakes, including beveled scarps and greater amount of offset along older deposits.

Because the scarp is the result of more than one earthquake, the site is not well suited for age determination by diffusion analyses. Scarp profiles (profiles 1 and 2) surveyed across the fault at the site show a displacement of between 2.3 and 2.5 m, respectively (Table 2; Electronic Supplement 2 [see footnote 1]). All three earthquakes postdate the stage II carbonate soil developed in the Qfi alluvium (Unit 1). Inset geomorphic relations indicate that the earthquakes occurred prior to deposition of Qfy fans that cut the Qfi and lacustrine deposits. Undeformed lacustrine deposits where the fault crosses Hwy 50 indicate that the last earthquake likely predates the late Pleistocene highstand of Lake Edwards. Thus, the three earthquakes occurred in the late Pleistocene and were characterized by interevent times sufficient enough to develop soils on the two older colluviums. The lack of carbonate development in the most recent earthquake colluvium suggests that it occurred in the latest Pleistocene.

Along the southeastern flank of the Desatoya Range, we mapped an ~20 km section of the fault north of State Highway 722. In the vicinity of Stalefish Creek, a 6–8-m-high scarp in bedrock projects across a Qfi surface, which is offset a similar amount (Electronic Supplement 3, Fig. ES 3.3 [see footnote 1]). The elevation of the scarp is slightly higher than the Lake Desatoya highstand shoreline elevation, but it projects northeast into the basin, where it has been covered by playette and prominent V-bar deposits. The observations support the occurrence of at least one late Pleistocene earthquake along the southeastern Desatoya range that occurred after the deposition of Qfi surfaces and prior to the highstand of Lake Desatoya.

Toiyabe Range

The north-northeast–trending Toiyabe Range is one of the longest (~170 km) and most topographically prominent ranges in central Nevada (Fig. 1B). Topographic relief from the highest peaks to the valley floor is around 1800 m. The range is a west-dipping horst block bound by active normal faults on both sides of the range. The western range front is a sharp linear escarpment characterized by large, well-developed, steep, triangular facets (Electronic Supplement 3, Fig. ES 3.4 [see footnote 1]). Older generations of facets extend to the crest of the range, and canyon mouths are typically deep, narrow, V-shaped notches in bedrock that extend upward into wineglass canyons. Between Highway 50 and Big Creek, large, steep, young alluvial fans are actively burying older alluvial surfaces along the range front, and scarps in alluvium are not observed. Directly south of Big Creek, an ~4-m-high fault scarp associated with a graben projects across an intermediate-aged surface west of the range front (Electronic Supplement 3, Fig. ES 3.4 [see footnote 1]). This scarp is beveled and likely represents more than one earthquake.

The eastern Toiyabe range front is characterized by a relatively continuous fault trace that is commonly buried by colluvium and young alluvial fans along the bedrock escarpment. The escarpment is characterized by wineglass canyons, triangular facets, and oversteepened basal slopes. Prominent scarps in Quaternary

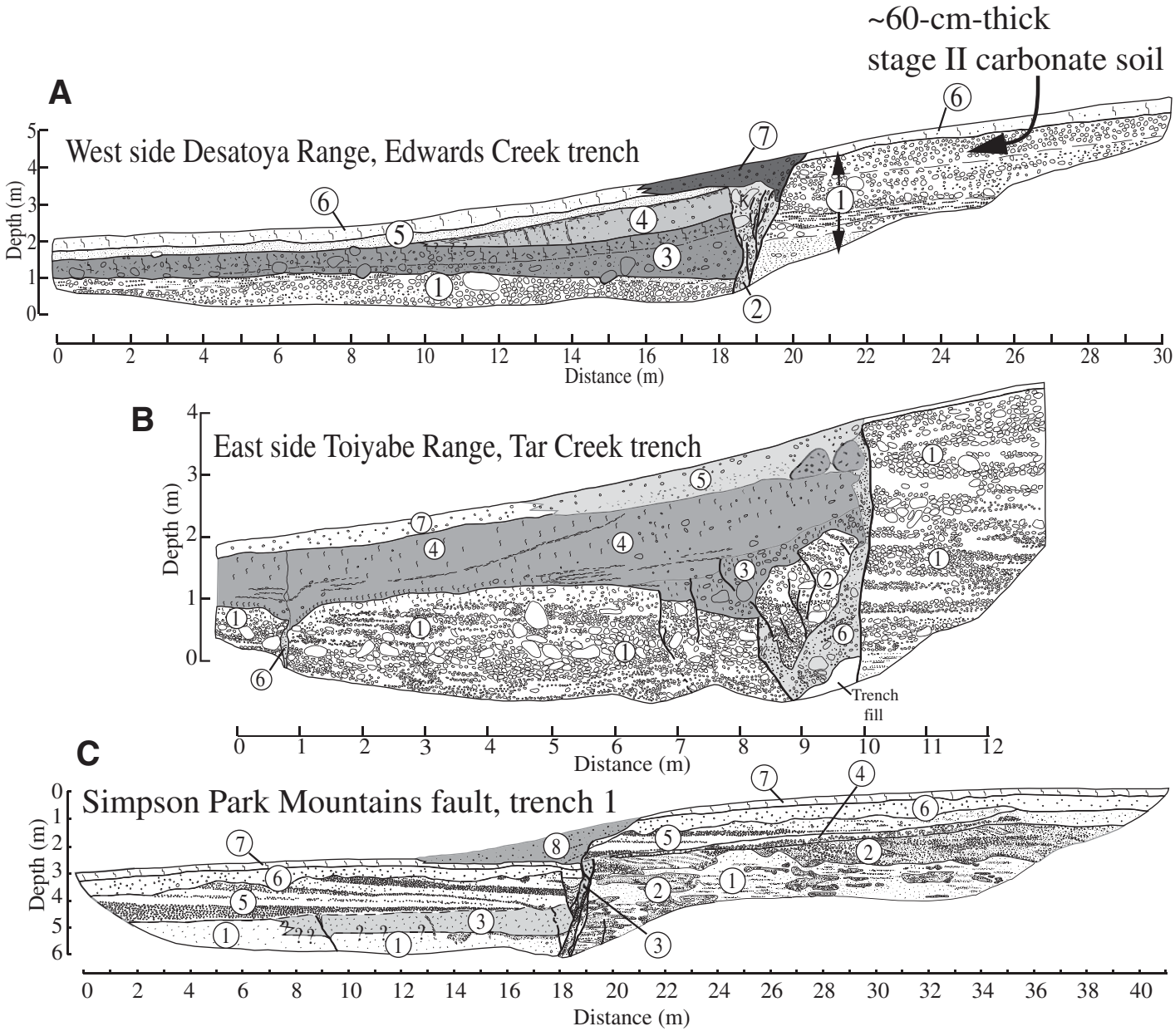

Figure 6. (A) Log of the western Desatoya Range fault trench west of Edwards Creek (39.48246°N, 116.69593°W) showing most recent earthquake colluvium (unit 7, black), penultimate colluvium (unit 4, light gray), and oldest earthquake colluvium (unit 3, dark gray). (B) Log of the Tar Creek trench (south wall) across the eastern Toiyabe Range fault located at 39.3352°N, 117.0219°W. Fault scarp–derived colluvium from the penultimate event is shaded dark gray. Most recent earthquake colluvium is shaded light gray. (C) Stratigraphic log of trench 1 along the Simpson Park Mountains fault located at 39.94087°N, 116.57371°W. Penultimate colluvium (unit 3) is shaded light gray, and most recent earthquake colluvium (unit 8) is shaded dark gray.

alluvium occur east of the range front along two ~5-km-long sections, including an area south of Kingston Canyon and the area between Santa Fe Creek and Highway 50. Detailed geologic mapping was conducted along the fault north of Santa Fe Creek, and a trench was excavated across a fault scarp in Qfi alluvium directly north of Tar Creek (Electronic Supplement 3, Figs. ES 3.4 and ES 3.5 [see footnote 1]).

A trench excavated across the northwestern trace at Tar Creek exposed an offset package of alluvial-fan gravels overlain by fault scarp colluvium (Fig. 6). The history of faulting exposed in the trench supports the occurrence of two surface-rupturing earthquakes that occurred after the deposition of the alluvial fan (unit 1). In the penultimate event, unit 1 was down-dropped across the fault, and unit 2 (a block of unit 1) was disrupted and back tilted into a graben (Fig. 6). Subsequent to the penultimate event, a fining-upward, eastward-thinning package of scarp colluvium (units 3 and 4) was deposited against the free face. By projecting the top of unit 1 on the hanging wall to the fault and measuring to the top of the penultimate colluvium, we determined that the penultimate event was associated with ~1.5 m of down-to-the-

southeast displacement. The most recent event occurred after the deposition of unit 4, based on separation of the penultimate colluvium from unit 1 across the fault, and 0.5–1-cm-thick carbonate-lined shears extending through units 2 and 3 that offset the base of unit 4. Based on loose consistency, randomly oriented clasts, and some remnant bedding, unit 6 is inferred to represent disrupted unit 1 material that mixed with surface deposits as fissure fill during the most recent event. Unit 5 represents scarp-derived colluvium associated with the most recent earthquake and consists of loose unconsolidated material and two relatively hard blocks adjacent to the fault. The blocks are interpreted to be pieces of unit 4 that rotated out of the fault zone during the most recent event. By measuring the vertical distance from the top of the penultimate colluvium to the top of unit 1 on the footwall, we determined that the most recent earthquake was associated with ~0.5 m of normal displacement. Sufficient time has elapsed since the earthquake for erosional processes to mute the expression of the event on the surface.

Surface-rupturing earthquakes recorded in the Tar Creek trench postdate the age of the Qfi deposit and associated soil cut by the fault. Soil descriptions at the site (Koehler, 2009) indicate that the hanging-wall and footwall slopes comprise the same surface and are characterized by a 22-cm-thick textural B horizon and stage II+ carbonate development (Birkeland, 1999). A scarp profile (profile 1) surveyed adjacent to the trench shows a cumulative vertical separation for the two events of 1.8 m (Table 2). Therefore, the two events are broadly constrained to after late middle to late Pleistocene and after formation of the stage II+ carbonate soil developed in the Qfi fan. The comparatively lesser amount of carbonate in the most recent event colluvium as compared to the penultimate colluvium suggests a latest Pleistocene age for the most recent event.

Simpson Park Range

The 72-km-long Simpson Park Mountains extend between the Toquima Range and Cortez Range in the south and north, respectively, and are bounded on the west flank by a normal fault (Fig. 1B; Electronic Supplement 3, Fig. ES 3.6 [see footnote 1]). South of Walti Hot Springs, the fault is characterized by well-defined facets and prominent vegetation, spring, and bedrock lineaments along the range front (Electronic Supplement 3, Fig. ES 3.7 [see footnote 1]). North of Walti Hot Springs, the fault transitions to several left-stepping traces that displace pluvial landforms related to pluvial Lake Gilbert and alluvial fans with scarps of 1 m to greater than 10 m, respectively (Electronic Supplement 3, Fig. ES 3.8 [see footnote 1]). Paleoseismic trenches were excavated across the fault at two sites. Here, we describe relations exposed in trench 1, which best illustrate the history of faulting along the range. Information pertaining to trench 2 is contained in Koehler (2009) and Electronic Supplement 3, Figure ES 3.9 (see footnote 1).

Trench 1 is located across an ~2-m-high scarp that offsets the highstand shoreline of pluvial Lake Gilbert, located ~4 km north of Walti Hot Springs (Electronic Supplement 3, Fig. ES 3.7 [see footnote 1]). A log of the trench exposure is shown on Figure 6. Stratigraphic and structural relations recorded in trench 1 support the occurrence of two surface-rupturing earthquakes that occurred after the deposition of units 1 and 2. The occurrence of the penultimate event is supported by the juxtaposition of units 1 and 2 against fault scarp colluvium (unit 3) that accumulated against the scarp and sheared lenses of units 1 and 2 within the 0.5-m-wide fault zone. The penultimate colluvium (unit 3) was exposed at the surface long enough to accumulate pedogenic carbonate and become well-cemented. The penultimate paleoscarp was eroded by wave processes during the late Pleistocene transgression of pluvial Lake Gilbert, and was eventually buried by beach deposits (unit 5). Subsequent to lake desiccation, a soil developed on the beach gravels (units 6 and 7). Units 5, 6, and 7 extend across the entire exposure and are correlated across the fault where they are offset ~1.75 m and form a west-facing scarp. The elevation of the soil on the footwall coincides with the 1750 m highstand elevation of pluvial Lake Gilbert (Mifflin and Wheat, 1979; Reheis, 2002). The scarp, offset strata, fissure fills in units 3 and 5, and fault scarp–derived colluvium (unit 8) that tapers away from the scarp are evidence for a second (most recent) paleoearthquake.

The highstand shoreline of pluvial Lake Gilbert (1750 m) is cut by the fault in several places (Electronic Supplement 3, Figs. ES 3.7 and ES 3.8 [see footnote 1]) and is correlated to the trench 1 site by elevation. The timing of the highstand is inferred to be latest Pleistocene, based on comparison of morphology and preservation of shore features, as well as correlation of soils to those of known Lahontan age (Koehler, 2009; Mifflin and Wheat, 1979; Adams and Wesnousky, 1999). Lake Lahontan reached its maximum extent at 13,070 ± 60 ^{14}C yr B.P. (15,475 ± 720 cal yr B.P.; Adams and Wesnousky, 1999; Benson and Thompson, 1987). Stratigraphic relations preserved in a gravel pit oriented oblique to the highstand beach berm in northern Grass Valley showing the Mazama tephra onlapping the lacustrine deposits indicate that the highstand predates the Mazama tephra (Koehler, 2009). Thus, the maximum limiting age for the most recent earthquake on the Simpson Park Mountains fault is latest Pleistocene.

Scarp profile 1 surveyed adjacent to trench 1 shows that the surface offset is identical to the offset of the base of unit 5 across the fault in the trench, indicating that the surface scarp was produced by a single earthquake (Table 2). The synthetic profile that best fits the observed profile is for an offset of 1.7 m and indicates the occurrence of an earthquake at 6.5 ka (Table 2; Electronic Supplement 2 [see footnote 1]). At trench 2, the diffusion analysis of profile 2 places the offset at 4.2 m and scarp formation at 9 ka (Table 2; Electronic Supplement 2 [see footnote 1]). Due to deposition on the hanging wall of trench 2, age estimation by diffusion modeling is not ideal. However, the slope of the diffusion curve for κt = 9 is a good fit with the footwall slope. As such, the age estimate for the scarp at trench 2 represents a first-order approximation and is not as reliable as the diffusion estimate at trench 1. Nonetheless, the two scarp profile ages for the most recent earthquake are consistent with the offset of latest Pleistocene lacustrine deposits of Lake Gilbert. Considering that some time was necessary to develop a soil on the beach gravels at trench 1 (units 6 and 7) prior to displacement, the age of the most recent earthquake is broadly constrained between latest Pleistocene and early Holocene. The close proximity and nearly continuous youthful scarps between the two trench sites suggest that the same earthquake is recorded at both sites. The penultimate event observed in trench 1 occurred prior to the highstand of Lake Gilbert and prior to the accumulation of carbonate in the penultimate colluvium (unit 3). Evidence for a penultimate event was not observed in trench 2, suggesting that it occurred prior to deposition of the fan or did not rupture as far south as the most recent event.

Toquima Range

The ~N20°E Toquima Range extends ~120 km from southwestern Monitor Valley in the south to the Simpson Park Mountains in the north (Fig. 1B; Electronic Supplement 3, Fig. ES 3.10 [see footnote 1]). The relief, dramatic eastern bedrock escarpment, and west tilt of the range are a result of long-term faulting along an east-dipping normal fault system. The fault is characterized by several major en echelon left steps that occur in the vicinity of Andrews Canyon and Potts Ranch (Electronic Supplement 3, Fig. ES 3.10 [see footnote 1]). The morphological expression of Quaternary faulting includes juxtaposition of bedrock and alluvial-fan sediments

along the range front, bedrock facets, wine glass canyons, scarps in Qfo and Qfi deposits, and wide grabens in alluvium.

Scarp profiles were surveyed across unbeveled scarps in Qfi alluvium in each of three sections mapped along the range, including scarps near Road Canyon (profile 1), Ikes Canyon (profile 2), and north of Dry Creek (profile 3) (Table 2; Electronic Supplements 2 and 3, Figs. ES 3.11, ES 3.12, and ES 3.13 [see footnote 1]). Diffusion analyses place the displacement at 1.87 and 1.1 m and the age of scarp formation at around 55 and 60.5 ka for profile 1 at Road Canyon and profile 2 at Ikes Canyon, respectively. North of Dry Creek, profile 3 matches a synthetic profile with an offset of 1.1 m and indicates an age of ca. 16 ka for the scarp. The diffusion analyses indicate that an earthquake occurred on the southern part of the Eastern Toquima Range fault system in the late Pleistocene, and a relatively younger event occurred along the northern section in the latest Pleistocene.

Monitor Range

The Monitor Range extends ~165 km from Kobeh Valley in the north to the vicinity of Hwy 6 in the south (Fig. 1B; Electronic Supplement 3, Fig. ES 3.10 [see footnote 1]). The range is a horst structure with a general trend of N20°E that has been elevated ~1 km from piedmont slopes along active faults that trend along the western and eastern range fronts. Prominent expression of faulting in Quaternary alluvium occurs north of Potts Ranch (western side), and within Little Fish Lake Valley (eastern side).

Along the western flank of the Monitor Range, two scarp profiles (profiles 1 and 2) were surveyed across a small scarp directly north and south of National Forest Road 004, west of Wallace Canyon (Electronic Supplement 3, Fig. ES 3.14 [see footnote 1]). The scarp is characterized by a smooth unbeveled profile and small displacement. Identical surface morphology and amounts of stream incision on the footwall and hanging-wall slopes indicate that the surfaces match across the fault, suggesting the scarp was produced by a single event. Diffusion analyses of the two profiles yield identical results. The best-fit synthetic profiles are associated with a vertical displacement of 0.85 m and suggest the occurrence of an earthquake along the Monitor Range fault ca. 44 ka (Table 2; Electronic Supplement 2 [see footnote 1]). At least one other subparallel trace cuts across the same surface and has similar scarp characteristics. Thus, the total amount of vertical offset during the late Pleistocene may be as large as ~1.7 m.

The eastern flank of the Monitor Range is characterized by a relatively continuous east-dipping range-front fault trace that extends the entire length of Little Fish Lake Valley and at least two Quaternary traces east of the range front (Electronic Supplement 3, Fig. ES 3.15 [see footnote 1]). Intermediate-aged alluvial fans (Qfi) along Tulle and Dobbin Creeks are displaced ~2 m, and young alluvial fans are not offset. The fault scarps in Qfi alluvium have rounded crests and similar field expression as scarps within Monitor Valley to the west. Additionally, the surface morphology of Qfi deposits cut by the fault is similar to other Qfi deposits throughout the study region, and is consistent with a late Pleistocene age. We infer that the last earthquake along the eastern flank of the Monitor Range occurred in the late Pleistocene.

Antelope Range

Extending from the northern end of Little Fish Lake Valley to the vicinity of Fenstermaker Wash, the Antelope Range represents a relatively short (~30 km) N5°E-trending east-tilted structural block (Fig. 1B; Electronic Supplement 3, Fig. ES 3.16 [see footnote 1]). Structural relief of ~1040 m occurs in the vicinity of Ninemile Peak and diminishes to the north and south. The western side of the range between Cabin Spring and the Mahogany Hills is characterized by steep topography, oversteepened triangular facets, and a range-bounding normal fault that offsets alluvial fans in canyon salients (Electronic Supplement 3, Fig. ES 3.17 [see footnote 1]). The fault is typically obscured by slope colluvium and characterized by an inflection in the slope that is visible when backlit by morning sunlight.

The history of faulting events along the Antelope Range fault is expressed well at the mouth of Wily Creek and illustrated in the photo and sketch of the site shown on Figure 7. Two intermediate-age alluvial-fan surfaces (Qfia and Qfib) with similar surficial characteristics are preserved above the scarp. The Qfib surface is inset ~1 m into the Qfia surface across a terrace riser. A well-rounded crest and an oversteepened base characterize the scarp in both surfaces. On the hanging wall, a lobe of Qfib extends to the south and buries the Qfia surface. The observations support the occurrence of at least three earthquakes. The first earthquake elevated the Qfia surface, which was subsequently incised by the Qfib fan. This caused the deposition of a cone-shaped lobe (Qfib) below the scarp in the Qfia surface. The penultimate event displaced both the Qfia and Qfib surfaces and was followed by a period of quiescence sufficient to diffuse the crest of the scarp. Based on similar surficial characteristics above and below the scarp on the Qfib surface, the main channel of Wily Creek then incised to a depth that prevented further deposition on the hanging wall after the penultimate event. The most recent event oversteepened the scarp across the base of both surfaces. A profile surveyed across the scarp (profile 1) shows a displacement of 3.7 m at the Wily Creek site (Table 2l Electronic Supplement 2 [see footnote 1]). The displacement

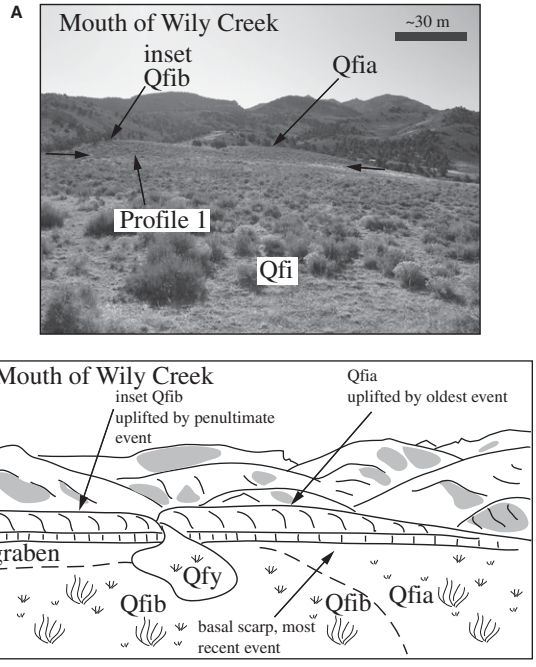

Figure 7. (A) Photograph of the Antelope Range fault at the mouth of Wily Creek. Fault extends between arrows. (B) Sketch of the fault at the mouth of Wily Creek showing evidence for three paleoearthquakes. See text for description of the earthquakes recorded in the fan stratigraphy.

is similar to the vertical separation of 3.0 m obtained from profile 2 surveyed across the scarp at the nearby Ninemile Canyon site (Table 2).

Along the northern section of the fault, ~4 km north of Fenstermaker Wash, two profiles were surveyed across a relatively smaller scarp in a Qfi deposit (profiles 3 and 4). This scarp is morphologically less degraded than the larger scarps south of Burly Canyon. Identical surficial characteristics on the hanging wall and footwall and the moderately sharp scarp crest morphology are consistent with a relatively youthful single rupture. The observed profiles for profiles 3 and 4 best fit synthetic profiles with vertical separations of 1.7 and 1.6 m, indicating scarp formation around 21 and 15 ka, respectively (Table 2; Electronic Supplement 2 [see footnote 1]). Thus, the combined observations indicate that the Antelope Range fault has experienced three earthquakes in the late Pleistocene and that the most recent event occurred in the latest Pleistocene around 15–21 k.y. ago. The maximum late Pleistocene displacement is ~3.7 m.

Fish Creek Range

The relatively narrow-tilted Fish Creek Range extends roughly N10°E for ~45 km between Cockalorum Wash and the vicinity of Lamoreux Canyon (Fig. 1B; Electronic Supplement 3, Figs. ES 3.16 and ES 3.18 [see footnote 1]). The bedrock is juxtaposed against Quaternary alluvial-fan sediments of Fish Creek Valley across an east-dipping range-front normal fault responsible for over 700 m of structural relief between the highest peaks and alluvial sediments. Directly south of Fish Creek Springs Road, the fault displaces a Qfi surface ~2.5 m. At this location, the hanging-wall and footwall surfaces have similar surficial characteristics, the scarp is smooth without bevels, and it is interpreted to be the result of a single earthquake. Synthetic profiles that best fit the observed profiles 1 and 2 are for a vertical separation of 2.7 and 2.3 m and indicate the occurrence of an earthquake rupture around 29.7 and 28 ka, respectively (Table 2; Electronic Supplement 2 [see footnote 1]).

Butte Range

The north-south–trending Butte Range extends ~78 km north from the northwestern end of Jakes Valley near U.S. Highway 50 to the headwaters of Long Valley Wash (Fig. 1B; Electronic Supplement 3, Fig. ES 3.19 [see footnote 1]). An active west-dipping normal fault bounds the western flank of the range. Features indicative of active deformation include well-developed triangular facets, uplifted pediment (QTp), and old alluvial-fan (Qfo) surfaces, scarps, and grabens. Within Long Valley, prominent late Pleistocene constructional beach and highstand shoreline features associated with pluvial Lake Hubbs are deposited on Qfi surfaces up to their maximum elevation of ~1920 m (Reheis, 1999) (Electronic Supplement 3, Fig. ES 3.20 [see footnote 1]).

A sketch of the south wall of a trench excavated across a 4.2 m west-facing scarp in Qfi materials ~6 km northeast of Dry Lake Well is shown in Figure 8. The trench site sits above the highstand shoreline of Lake Hubbs, which is not displaced by the fault. Directly south of the site, the Qfi surface has been inset >20 m by a Qfy surface that is also not offset. The trench stratigraphy records at least three earthquakes that postdate the deposition of the fan gravels (unit 1). The oldest earthquake is recorded by the deposition of colluvial material (unit 2) within the graben. The development of a soil and carbonate cementation indicates that unit 2 was exposed at the surface for many tens of thousands of years. Several faults extend from the base of the trench and appear to terminate at carbonate stringers within unit 2. Accumulation of a second package of colluvial material, unit 3, and faults that cut unit 2 but do not extend into unit 3 provide evidence for the penultimate earthquake. Evidence for the most recent earthquake includes a 1.5-m-wide graben at the scarp that cuts units 2 and 3, a set of fractures and fissure fills that cut units 2 and 3, and the accumulation of fault scarp colluvium and graben-fill material (unit 4).

Five fault scarp profiles were surveyed across scarps in Qfi alluvium (Table 2; Electronic Supplements 2 and 3, Fig. ES 3.20 [see footnote 1]). Profiles 1 and 2 were surveyed across an unbeveled fault scarp in a Qfi surface at the mouth of an unnamed stream ~4.6 km north of the trench. The scarp is inferred to be the result of a single earthquake based on the youthful morphology of the fan, relatively small offset, and matching surfaces across the fault. Profiles 1 and 2 best match synthetic profiles with offsets between 0.95 and 1.3 m and indicate an age for the most recent earthquake of between 18 and 22 ka (Table 2; Electronic Supplement 2 [see footnote 1]). At the trench site, the scarp is clearly related to multiple events and is not ideal for diffusion analysis. This is confirmed by the poor root mean square (RMS) misfit plots associated with attempts to model the age of the scarp (profiles 3 and 4), which are not discussed further (Table 2; Electronic Supplement 2 [see footnote 1]). The vertical separation at the trench site of 4.2 and 4.4 m indicated by profiles 3 and 4, respectively, is the cumulative displacement for the last three events (Table 2). Profile 5 was surveyed across a large scarp at the apex of a Qfi surface ~1.6 km south of the trench. This scarp is characterized by a degraded crest, oversteepened base, and an ~1-m-deep graben, indicating that it was formed by multiple events and is not appropriate for diffusion analysis. Profile 5 shows a displacement of 5.3 m, which is inferred to be the cumulative late Pleistocene displacement (Table 2).

All three earthquakes occurred prior to the latest Pleistocene highstand of pluvial Lake Hubbs and after the deposition of the Qfi surface, which is inferred to be late middle to late Pleistocene in age based on soil development. The continuity of the soil from the hanging wall across the top of unit 2 within the graben suggests that the oldest earthquake occurred shortly after the deposition of the surface. Based on the diffusion analyses (profiles 1 and 2), the most recent earthquake occurred around 20 ka. The earthquake chronology is consistent with wave-modified fault scarps, undeformed late Pleistocene lacustrine shoreline features, and well-developed alluvial-fan soils.

Egan Range

The northern Egan Range extends ~53 km from the city of Ely to the Cherry Creek Range and has a north-south trend with sinuous form in map view (Fig. 1B; Electronic Supplement 3, Fig. ES 3.21 [see footnote 1]). Active normal faulting along the eastern range front has uplifted pediment surfaces and displaced Qfi and Qfo surfaces.

A trench was sited across a 1.3-m-high scarp on a Qfi surface ~1 km south of Log Canyon. A log of the exposure is shown on Figure 8. The trench exposed alluvial-fan sediments (unit 1) faulted across an ~2-m-wide fissure. A distinct alluvial interbed, unit 2, may correlate across the fault. An eastward-thinning colluvial deposit (unit 4) fills the fissure and buries unit 1 on the hanging wall. A 40–80-cm-thick 2Bkm soil horizon with stage II to II+ carbonate development has developed into the entire exposure. The stratigraphy is interpreted to record one paleoearthquake, based on a similar offset of unit 2 measured at the fault to the surface offset, and the presence of a single colluvial wedge deposit (Fig. 8).

The continuity of the carbonate soil across the entire exposure indicates that the earthquake and the accumulation of the colluvium occurred prior to any significant development of the soil. Thus, the earthquake likely occurred near the time of surface abandonment and may have contributed to abandonment by altering base level. Stratigraphic relations from the trench and the similarity of the footwall and hanging-wall soils indicate that the scarp is the result of a single displacement, and surfaces at the trench site match

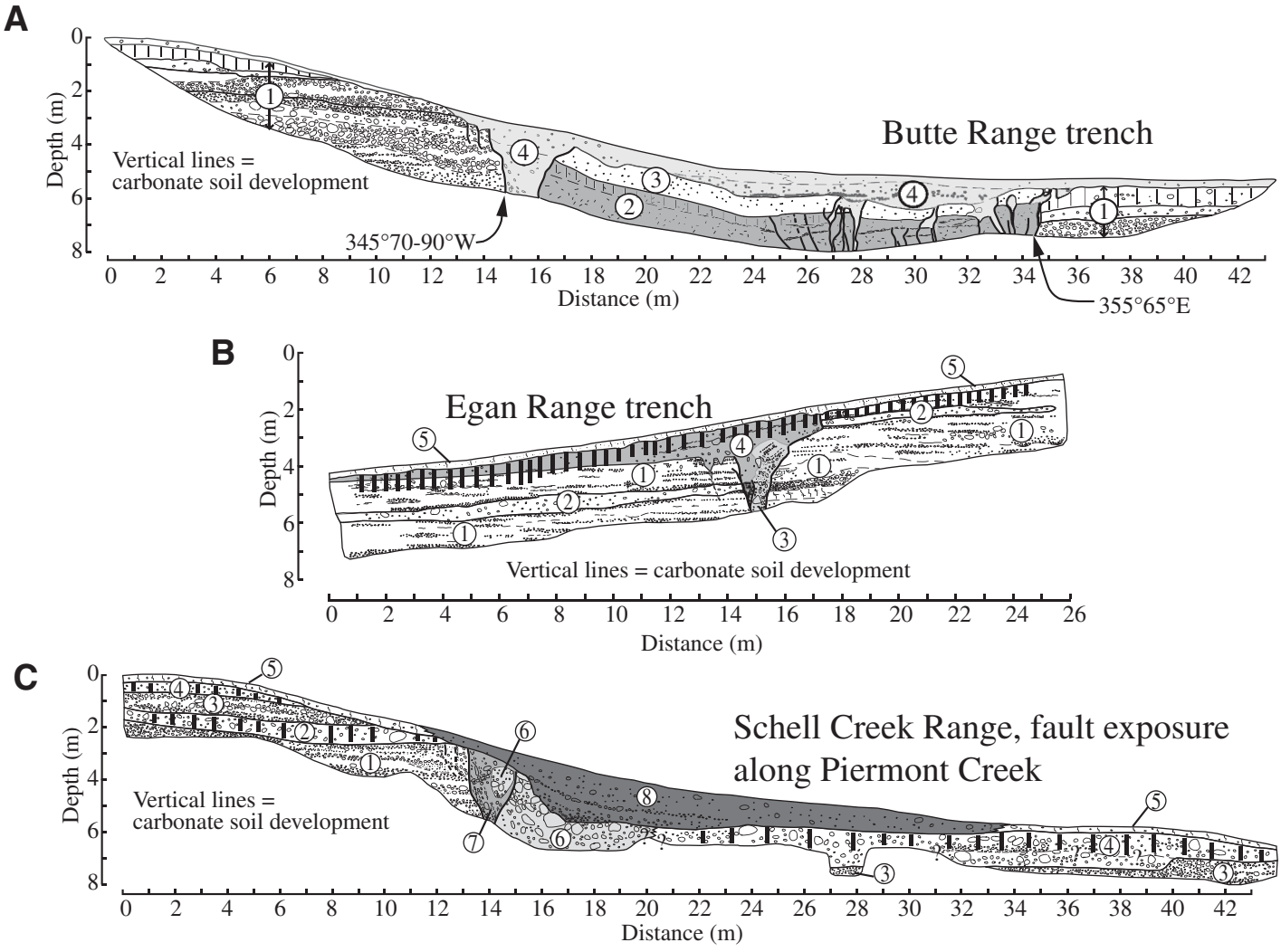

Figure 8. (A) Sketch of trench exposure along the Butte Range fault zone located at 39.73471°N, 115.3257°W. Graben-fill deposits represent three earthquakes: oldest (unit 2) shaded dark gray, penultimate (unit 3), and youngest (unit 4) shaded light gray. (B) Log of the Egan Range fault exposure located at 39.67563°N, 114.82656°W. Fault scarp–derived colluvium (unit 4, dark gray) indicates the scarp was formed by a single event. (C) Log of the Piermont Creek natural exposure of the Schell Creek Range fault. Exposure is located at 39.48886°N, 114.53503°W. Penultimate colluviums (unit 6) are shaded light gray. Most recent earthquake colluvium (unit 8) is shaded dark gray.

across the fault. Synthetic profiles best fit the observed profiles 1 and 2 with an offset of 1.3 m and indicate the occurrence of an earthquake between 42 and 60 ka, respectively (Table 2; Electronic Supplement 2 [see footnote 1]). Profiles 3 and 4 across a scarp in Qfi alluvium south of the trench are not ideally suited for diffusion analyses due to deposition on the hanging wall, but they indicate a late Pleistocene vertical separation of 2.2 m (Table 2). The trench observations indicate that an earthquake ruptured the Egan Range fault in the late Pleistocene. The timing of this event is consistent with the gentle gradient and smooth, subdued morphology of the scarp, the stage II to II+ carbonate soil developed across the exposure, and the diffusion result.

Schell Creek Range

The northern Schell Creek Range extends north-south for ~105 km between the vicinity of Majors Place along Highway 50 and the Antelope Range (Fig. 1B; Electronic Supplement 3, Fig. ES 3.21 [see footnote 1]). The topographic escarpment along the east side of the range is a product of long-term active normal faulting that has uplifted the crest of the range between 1.3 and 1.6 km. Tectonic geomorphic features include sharp oversteepened triangular facets, scarps in Quaternary alluvium, and greater amounts of offset along progressively older Quaternary surfaces (Electronic Supplement 3, Figs. ES 3.23 and ES 3.24 [see footnote 1]). Prominent shorelines associated with pluvial Lake Spring fringe the basin at 1759 m elevation (Reheis, 1999), and a suite of large recessional shorelines flanks the north end of the valley.

In the vicinity of Bastian Creek Ranch, the fault trends oblique to and cuts a Lake Spring recessional shoreline, and it is characterized by short overlapping traces, an alignment of trees, an ~1-m-high scarp, and multiple springs (Electronic Supplement 3, Fig. ES 3.23 [see footnote 1]). Young fan surfaces (Qfy) that are inset into Qfi deposits and shoreline features are generally not offset by the fault. Along the southern side of the Cleve Creek fan, the fault displaces a large, deeply dissected old alluvial-fan surface ~12–14 m (Electronic Supplement 3,

Fig. ES 3.25 [see footnote 1]). Within this surface, Koehler (2009) described a buried Btk soil horizon with laminated carbonate matrix and thick carbonate coats surrounding clasts consistent with stage III+ to IV carbonate development. The soil suggests that the surface is greater than several hundred thousand years old and has experienced multiple earthquakes.

Across the Cleve Creek fan, the fault is expressed as two subparallel traces that each offset the Qfi surface with scarps ~1 m high (Electronic Supplement 3, Fig. ES 3.25 [see footnote 1]). Younger elements of the Cleve Creek fan (Qfy) are not offset. Two trenches across the eastern and western traces of the fault at Cleve Creek exposure provide evidence for one earthquake displacement that broke a gravel surface capped by a 30–40-cm-thick 2Btk horizon with stage II carbonate development (Koehler, 2009). Surface map relations south of Cleve Creek that show displaced shorelines near Bastian Creek Ranch indicate that an earthquake occurred after the desiccation of pluvial Lake Spring. It is thus possible that the event recorded in the trench exposures occurred in the latest Pleistocene, after ca. 13 ka. Profiles 1, 2, 3, and 4 indicate that the combined vertical separation is on the order of 1.75 m across the two traces (Table 2).

At Piermont Creek, the fault steps away from the range front and is expressed as several short stepping strands that have preserved a Qfo surface and displaced a Qfi surface with scarps up to 4–5 m (Electronic Supplement 3, Fig. ES 3.24 [see footnote 1]). A log of a natural exposure of the fault at Piermont Creek is shown on Figure 8. The exposure provides evidence for at least two surface-rupturing earthquakes. A fault zone cuts units 1–5, which correlate across the fault zone and are back tilted. Unit 6 is interpreted to be either original stratigraphy that buckled and rotated into accommodation space within a graben or colluvium that accumulated after the penultimate event. During the most recent event, a 2-m-wide fissure opened adjacent to the fault and was filled with loose sediment (unit 7). The fissure was subsequently buried by a thick package of unconsolidated fault scarp–derived colluvium (unit 8). Soil is poorly developed in the colluvium, and it is characterized by a lack of pedogenic carbonate and no obvious horizonation.

The hanging-wall and footwall slopes have identical surficial characteristics across the scarp. The thickness of the colluvial wedge (~2.5 m) represents the majority of the scarp height (3.7 m), from which we infer that the scarp related to previous events was largely diffused and the scarp was primarily created by the most recent earthquake. Application of diffusion analysis to profiles 5, 6, and 7 adjacent to and near the trench places the vertical separation and age of scarp formation at ~3.85 m, 3.7 m, and 3.6 m, and 30, 35, and 32 ka, respectively (Table 2; Electronic Supplement 2 [see footnote 1]). The estimated age is consistent with or perhaps a bit older than that reflected by the limited soil development in the colluvium.

Taken together, the results from Piermont Creek and Cleve Creek suggest that the Schell Creek Range fault has generated at least one latest Pleistocene earthquake and a penultimate event several tens of thousands of years prior. Based on a less-developed soil at Cleve Creek, the Cleve Creek fan is interpreted to be younger than the Piermont Creek fan and does not record the penultimate event. Although the late Pleistocene highstand of pluvial Lake Spring is inferred to have been contemporaneous with the highstand of Lake Lahontan (Reheis, 1999; Mifflin and Wheat, 1979), it has not been directly dated. Therefore, given the uncertainties in the age of the highstand, uncertainties inherent in diffusion analysis, and the possibility that the scarp height at Piermont Creek may be due to more than one event, it is permissible that the same latest Pleistocene event created the scarps at Cleve Creek and Piermont Creek. Alternatively, considering the 28 km distance between the two sites, the fault may have ruptured around 30 ka near Piermont Creek and after ca. 13 ka near Cleve Creek. In either case, the relations point to at least one and likely two earthquakes in the late Pleistocene along the Schell Creek range front.

DISCUSSION AND CONCLUSIONS

Regional Paleoseismic Patterns and Extension Rate

A synopsis of the limits placed on the timing of surface-rupturing earthquakes along each of the ranges studied is provided in Table 1. Information on the age of surface ruptures reported by others for faults in the Walker Lane and Central Nevada seismic belt and in Utah and used for context in this study is detailed in Koehler (2009), Wesnousky et al. (2005), and Hecker (1993). The history of paleoseismic displacements garnered in this study is combined with those of others in the form of a space-time diagram in Figure 9. Collectively, the data represent a paleoseismic transect that spans the entire Great Basin from the Sierra Nevada to the Wasatch front, and we use it to discuss the pattern of late Pleistocene strain release, as well as the distribution and rate of occurrence of paleoearthquakes across the region.

Inspection of Figure 9 and Table 1 indicates that south of 40°N latitude, a greater number of paleoearthquakes and shorter recurrence intervals characterize the margins of the Great Basin, while fewer earthquakes and longer recurrence intervals are typical for faults in the interior. For example, trench studies indicate at least four post–ca. 15 ka earthquakes along the Pyramid Lake fault in the northern Walker Lane (Briggs and Wesnousky, 2004) and at least three Holocene events along the Nephi segment of the southern Wasatch fault in the Intermountain seismic belt (Jackson, 1991; Schwartz et al., 1983). Trench studies in the interior of the Great Basin indicate recurrence intervals of several tens of thousands of years (Crone et al., 2006; Machette et al., 2005; Wesnousky et al., 2005). The observations are similar to the pattern of deformation documented geologically across the Great Basin north of the 40th parallel (Wesnousky et al., 2005) and geodetically across the region (Chang et al., 2006; Hammond and Thatcher, 2004; Kreemer et al., 2009; Thatcher et al., 1999; Bennett et al., 2003). The pattern is also consistent with dense seismicity within the Walker Lane, Central Nevada seismic belt, and Intermountain seismic belt and diffuse seismicity within the interior of the Great Basin (Figs. 1A and 1B) (Pancha et al., 2006; http://quake.geo.berkeley.edu/anss/catalog-search.html). Taken together, the spatial distribution of background seismicity and loci of increased geodetic strain are similarly reflected in the observation that the recurrence rate of surface-rupturing earthquakes over the late Pleistocene to present day is greater along the margins than within the interior of the Great Basin. Furthermore, although paleoseismic studies along the margins of the Great Basin indicate similar paleoearthquake offsets (e.g., Ramelli et al., 1999; Schwartz et al., 1983) to those observed in the interior, the steeper range-front morphology and slightly greater elevation of the Sierra Nevada and the Wasatch Ranges suggest greater cumulative late Pleistocene displacement.

The rate of extension between the Central Nevada seismic belt and the Wasatch Front can be estimated based on the observed late Pleistocene vertical displacements, calculated horizontal displacements (Fig. 5), and the time period over which the offset occurred. Based on scarp diffusion and Quaternary stratigraphic relations, displacements for the last ~60 k.y. and ~20 k.y. are cataloged in Tables 3 and 4, respectively. Earthquake displacements used in the extension rate calculation all postdate abandonment of their respective Qfi fan surfaces. The ages of the Qfi fan surfaces provide a maximum age for the ruptures, and they were used to independently verify the extension rates calculated using scarp diffusion ages. Based on regionally similar surface morphology, degree of incision, and soil development characterized by stage II to II+ carbonate

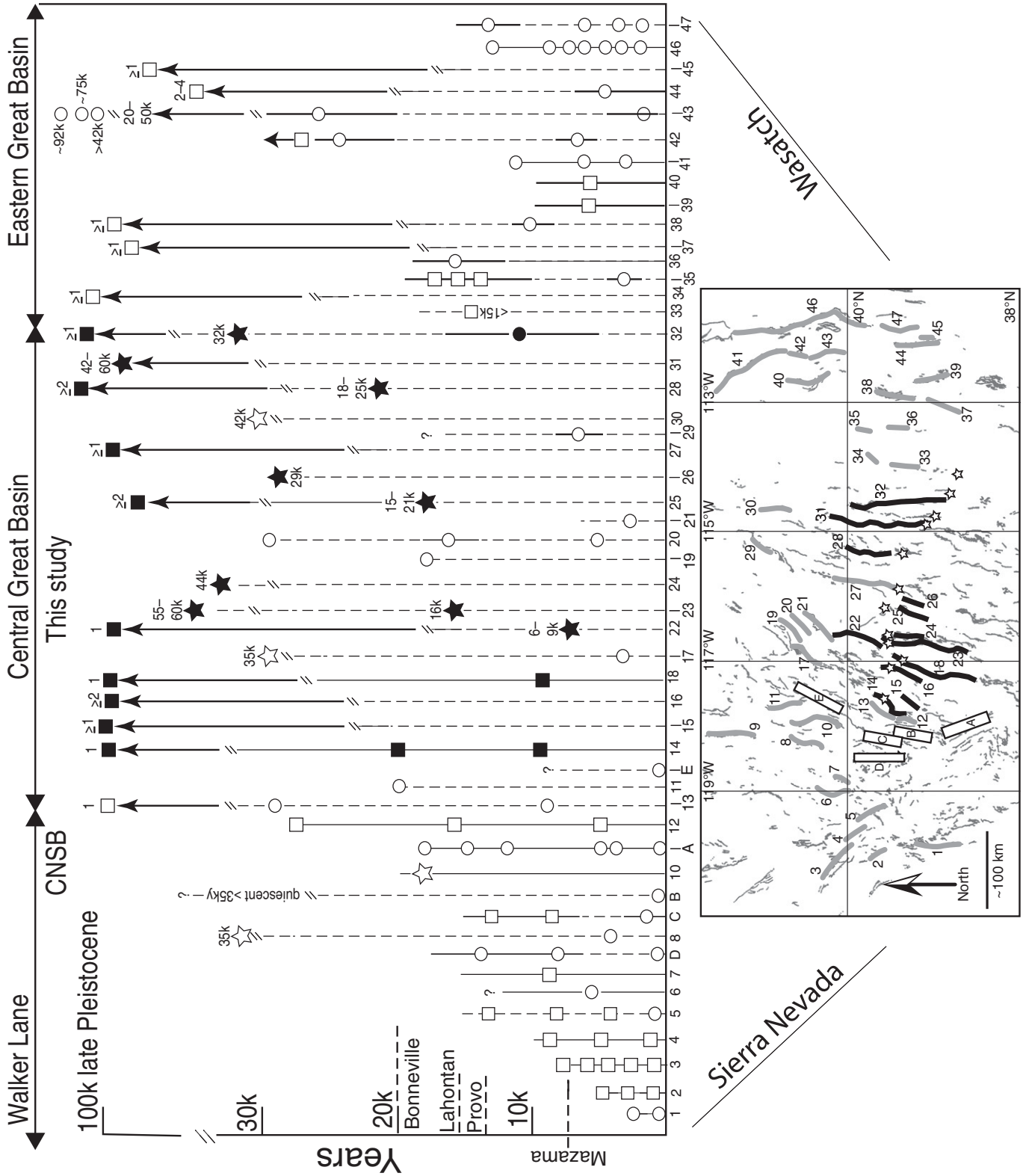

Figure 9.

Figure 9. Space-time diagram showing late Pleistocene earthquake history across the Great Basin from the Sierra Nevada to the Wasatch Mountains between 38.5°N and 40.5°N latitude, including information from previous studies in Utah and Nevada. The vertical axis is time, and the horizontal axis is distance, expanded but roughly scaled to the map of the northern Great Basin below. Solid black symbols are earthquakes investigated in this study, and open symbols indicate earthquakes studied by others. The location of each symbol represents the age of an earthquake surface rupture. Stars indicate ages of earthquakes estimated by scarp diffusion analyses, circles indicate the age of earthquakes determined from trench studies, and squares indicate the number of events that have occurred subsequent to a particular age (plotted evenly over the age range). Solid black vertical lines represent the range in age for a particular event. Dashed vertical lines indicate the approximate time interval for which observations are available. Tag lines are broken with a diagonal line symbol where events occurred earlier than the time scale. Earthquake histories for each fault on the space-time diagram are keyed to the map using number and letter labels. On the map, faults that are the focus of this study and faults studied by others are colored black and gray, respectively. Paleoseismic information for the faults is shown on Table 1 and summarized in Wesnousky et al. (2005), Koehler (2009), and Hecker (1993). CNSB—central Nevada seismic belt. Faults: 1—Genoa, 2—Peavine Peak, 3—Honey Lake, 4—Warm Springs, 5—Pyramid Lake, 6—Shawaves, 7—Bradys, 8—Humboldt, 9—Santa Rosa, 10—Stillwater (east side), 11—Sonoma, 12—East gate, 13—Clan Alpine, 14—Desatoya (west side), 15—Desatoya (east side), 16—Toiyabe (west side), 17—Shoshone, 18—Toiyabe (east side), 19—Tuscarora-Malpais, 20—Dry Hills, 21—Cortez, 22—Simpson Park, 23—Toquima south and north (Hickison Summit), 24—Monitor, 25—Antelope, 26—Fish Creek, 27—Diamond (east side), 28—Butte, 29—East Humboldt, 30—Pequops, 31—Egan, 32—Schell Creek, 33—Snake Valley, 34—Deep Creek, 35—Fish Springs, 36—House Range, 37—Crickett Mountains, 38—Drum Mountains, 39—Clear Lake, 40—Stansbury, 41—E Great Salt Lake, 42—Oquirrh, 43—S Oquirrh, 44—Little/Scipio Valley, 45—Japanese Valley, 46 and 47—Wasatch. Historic ruptures (CNSB) shown as rectangular boxes include: (A) 1932 M 7.2 Cedar Mountain, (B) 1954 M 7.2 Fairview Peak, (C) 1954 M 6.8 Dixie Valley/Sand Spring, (D) 1954 M 6.8/6.6 Rainbow Mountain and Stillwater, and (E) 1915 M 7.7 Pleasant Valley.

development, the Qfi surfaces are broadly constrained to between ca. 50 and 175 ka. This age range encompasses the timing of regional intervals of fan aggradation inferred to have occurred during OIS 4–OIS 3 (57–70 ka) and OIS 6–OIS 5 (ca. 130 ka) climatic transitions (Eppes et al., 2003; Lisiecki and Raymo, 2005).

The total amount of measured vertical displacement between the Central Nevada seismic belt and the Wasatch fault is 91.3 m and 35.4 m, over the last ~60 k.y. and ~20 k.y., respectively (Tables 3 and 4). The calculated total net east-west horizontal extension over the same time periods is ~48.4 m and 19.3 m, respectively. Averaging these values over the time periods that the displacements occurred yields long-term extension rates of 48.4 m/60 k.y. = 0.8 mm/yr and 19.3 m/20 k.y. = 1.0 mm/yr. Dividing the total east-west extension (48.4 m) by the possible range of ages for the displaced surfaces (50–175 ka) results in an extension rate of 0.3–1.0 mm/yr, consistent with our result. Thus, a first-order estimate of the regional long-term extension rate across the Great Basin (0.8–1.0 mm/yr) is reasonable and has been operative over the late Pleistocene to present. The extension rate is similar to the rate determined for the area north of the 40th parallel (Wesnousky et al., 2005), suggesting that extensional strain release rates in the interior of the Great Basin are similar across the latitudes of 38.5°N to 41°N across the region.

The extension rate reported here encompasses geologic observations across the entire region but represents a minimum estimate. Unrecognized late Pleistocene slip may have occurred along range fronts that have moderate tectonic geomorphology but lack scarps in alluvium, including the eastern Shoshone, western Diamond, western White Pine, western Egan, and western Snake Ranges. However, if we account for the possibility of 1–4 m of slip on all of these ranges, the extension rate only increases by ~0.2 mm/yr. Vertical separations for scarps that were not trenched may have an unknown amount of deposition on the hanging wall, and they represent a minimum estimate of the offset. Based on trench observations across the region, hanging-wall deposition is generally less than 1 m. Thus, the underestimation of vertical separation of ~1 m at these sites has little effect on the extension rate averaged across the region. An unknown amount of extension may be related to non-surface-rupturing earthquakes, small scarps removed by erosion, fault traces within bedrock, and/or traces associated with half grabens within valleys that are now buried by basin-fill deposits. The analysis assumes that faults dip at 60° and displacements measured at the surface are representative of displacement at depth. The extension rate would be three times faster than our minimum estimate if the faults actually dip ~30°; however, this seems unlikely based on historical earthquake mechanisms that suggests steeper dips (Doser, 1985, 1986).

The central Great Basin has previously been modeled as a rigid geodetic "microplate" extending east-west as a block with no significant internal deformation (Hammond and Thatcher, 2005, 2004; Thatcher et al., 1999; Bennett et al., 2003). This was due primarily to the resolution and density of previous campaign GPS studies. Recent geodetic modeling efforts incorporating results from high-precision GPS data associated with the EarthScope array are beginning to better characterize crustal deformation in the region. In a study of the 21 February 2008 Mw 6.0 earthquake, Hammond et al. (2010) found a gradient in velocity of ~1 mm/yr over a width of ~250 km across the interior of the Great Basin and a maximum horizontal crustal extension direction of N59°W. Thus, withstanding the uncertainties, the long-term (geologic) net east-west extension rate of 0.8–1.0 mm/yr calculated here is, to first order, similar to short-term crustal velocities measured geodetically (Hammond et al., 2010; Thatcher et al., 1999; Bennett et al., 2003). The timing and distribution of late Pleistocene earthquake ruptures in the central Great Basin indicate that deformation is characterized by slow, distributed extension partitioned on faults with no obvious clustering in time and space. This diffuse pattern of strain release indicates internal deformation within the Great Basin and defines the style of deformation along the eastern margin of the >1000-km-wide Pacific–North American plate boundary.

ACKNOWLEDGMENTS

This research was supported by National Science Foundation award EAR-0509672. Additional support to Koehler was provided by the Graduate Student Research Grants Program of the Geological Society of America and the Jonathan O. Davis Scholarship of the Desert Research Institute. Field assistance from the following is greatly appreciated: Humboldt State University field camp (2006, 2007), University of Nevada, Reno Quaternary mapping class (2005, 2006), Joanna Redwine, Jayne Bormann, Mark Hemphill-Haley, Jon Caskey, Paul Sundberg, Jason Buck, and Alex Sarmiento. Chuck Lane of the Bureau of Land Management, Battle Mountain District, was invaluable in obtaining excavation permits. The manuscript benefited from thoughtful comments from Frank Pazzaglia, Enrico Tavarnelli, and an anonymous reviewer. This is Center for Neotectonic Studies contribution 54.

REFERENCES CITED

Adams, K.D., and Wesnousky, S.G., 1998, Shoreline processes and the age of the Lake Lahontan highstand in the Jessup embayment, Nevada: Geological Society of America Bulletin, v. 110, no. 10, p. 1318–1332, doi: 10.1130/0016-7606(1998)110<1318:SPATAO>2.3.CO;2.

Adams, K.D., and Wesnousky, S.G., 1999, The Lake Lahontan Highstand: Age, surficial characteristics, soil development, and regional shoreline correlation: Geomorphology, v. 30, p. 357–392, doi: 10.1016/S0169-555X(99)00031-8.

Allmendinger, R.W., 1992, Fold and thrust tectonics of the western United States exclusive of the accreted terranes, *in* Burchfiel, B.C., Lipman, P.W., and Zoback, M.L., eds., The Cordilleran Orogen: Conterminous U.S.: Boulder, Colorado, Geological Society of America, Geology of North America, v. G3, p. 583–607.

Anderson, E.M., 1951, The Dynamics of Faulting: Edinburgh, Oliver and Boyd, 206 p.

Anderson and Bucknam, 1979, Map of Fault Scarps in Unconsolidated Sediments, Richfield 1° × 2° Quadrangle, Utah: U.S. Geological Survey Open-File Report 79–1236, 15 p., scale 1:250,000.

Argus, D.F., and Gordon, R.G., 1991, Current Sierra Nevada–North America motion from very long baseline interferometry: Implications for the kinematics of the western United States: Geology, v. 19, no. 11, p. 1085–1088, doi: 10.1130/0091-7613(1991)019<1085:CSNNAM>2.3.CO;2.

Armstrong, R.L., and Ward, P., 1991, Evolving geographic patterns of Cenozoic magmatism in the North American Cordillera: The temporal and spatial association of magmatism and metamorphic core complexes: Journal of Geophysical Research, v. 96, no. B8, p. 13,201–13,224, doi: 10.1029/91JB00412.

Atwater, T., 1970, Implication of plate tectonics for Cenozoic tectonic evolution for western North America: Geological Society of America Bulletin, v. 81, p. 3513–3536, doi: 10.1130/0016-7606(1970)81[3513:IOPTFT]2.0.CO;2.

Bachman, G.O., and Machette, M.N., 1977, Calcic Soils and Calcretes in the Southwestern United States: U.S. Geological Survey Open-File Report 77–794, 163 p.

Bartley, J.M., Axen, G.J., Taylor, W.J., and Fryxell, J.E., 1988, Cenozoic tectonics of a transect through eastern Nevada near 38°N latitude, *in* Weide, D.L., and Faber, M.L., eds., This Extended Land; Geological Journeys in the Southern Basin and Range: Geological Society of America, Cordilleran Section, Field Trip Guidebook: Las Vegas, Nevada, Department of Geoscience, University of Nevada, p. 1–20.

Bell, J.W., and Katzer, T., 1990, Timing of late Quaternary faulting in the 1954 Dixie Valley earthquake area, central Nevada: Geology, v. 18, p. 622–625, doi: 10.1130/0091-7613(1990)018<0622:TOLQFI>2.3.CO;2.

Bell, J.W., dePolo, C.M., Ramelli, A.R., Sarna-Wojcicki, A.M., and Meyer, C.E., 1999, Surface faulting and paleoseismic history of the 1932 Cedar Mountain earthquake area, west-central Nevada, and implications for modern tectonics in the Walker Lane: Geological Society of America Bulletin, v. 111, p. 791–807, doi: 10.1130/0016-7606(1999)111<0791:SFAPHO>2.3.CO;2.

Bell, J.W., Caskey, S.J., Ramelli, A.R., and Guerrieri, L., 2004, Pattern and rates of faulting in the Central Nevada seismic belt and paleoseismic evidence for prior belt-like behavior: Bulletin of the Seismological Society of America, v. 94, p. 1229–1254, doi: 10.1785/012003226.

Bennett, R.A., Wernicke, B.P., and Davis, J.L., 1998, Continuous GPS measurements of contemporary deformation across the northern Basin and Range Province: Geophysical Research Letters, v. 25, no. 4, p. 563–566, doi: 10.1029/98GL00128.

Bennett, R.A., Davis, J.L., and Wernicke, B.P., 1999, Present-day pattern of Cordilleran deformation in the western United States: Geology, v. 27, no. 4, p. 371–374, doi: 10.1130/0091-7613(1999)027<0371:PDPOCD>2.3.CO;2.

Bennett, R.A., Wernicke, B.P., Niemi, N.A., Friedrich, A.M., and Davis, J.L., 2003, Contemporary strain rates in the northern Basin and Range Province from GPS data: Tectonics, v. 22, no. 2, p. 1008, doi: 10.1029/2001TC001355.

Benson, L.V., and Thompson, R.S., 1987, Lake-level variation in the Lahontan basin for the last 50,000 years: Quaternary Research, v. 28, p. 69–85, doi: 10.1016/0033-5894(87)90034-2.

Birkeland, P., 1999, Soils and Geomorphology: Oxford, UK, Oxford University Press, 432 p.

Birkeland, P.W., Machette, M.N., and Haller, K.M., 1991, Soils as a Tool for Applied Quaternary Geology; Manual for a Short Course, May 30–June 1, 1990: Utah Geological and Mineral Survey Miscellaneous Publication Series, 63 p.

Briggs, R.W., and Wesnousky, S.G., 2004, Late Pleistocene fault slip rate, earthquake recurrence, and recency of slip along the Pyramid Lake fault zone, northern Walker Lane, United States: Journal of Geophysical Research, v. 109, p. B08402, doi: 10.1029/2003JB002717.

Bucknam, R.C., and Anderson, R.E., 1979a, Map of Fault Scarps on Unconsolidated Sediments, Delta 10 × 20 Quadrangle, Utah: U.S. Geological Survey Open-file Report 79–366, 21 p., scale 1:250,000.

Bucknam, R.C., and Anderson, R.E., 1979b, Estimation of fault-scarp ages from a scarp-height-slope-angle relationship: Geology, v. 7, p. 11–14, doi: 10.1130/0091-7613(1979)7<11:EOFAFA>2.0.CO;2.

Bucknam, R.C., Crone, A.J., and Machette, M.N., 1989, Characteristics of active faults, *in* Jacobson, J.L., ed., National Earthquake Hazards Reduction Program; Summaries of Technical Reports, Volume XXVIII: U.S. Geological Survey Open-File Report 89–453, p. 117.

Caskey, S.J., Bell, J.W., Slemmons, D.B., and Ramelli, A.R., 2000, Historical surface faulting and paleoseismology of the Central Nevada seismic belt, *in* Lageson, D.R., Peters, S.G., and Lahren, M.M., eds., Great Basin and Sierra Nevada, Geological Society of America Field Guide, Volume 2: Boulder, Colorado, Geological Society of America, p. 23–44.

Caskey, S.J., Bell, J.W., and Wesnousky, S.G., 2004, Historic surface faulting and paleoseismicity in the area of the 1954 Rainbow Mountain–Stillwater earthquake sequence: Bulletin of the Seismological Society of America, v. 94, p. 1255–1275, doi: 10.1785/012003012.

Chang, Wu-Lung, Smith, R.B., Meertens, C.M., and Harris, R.A., 2006, Contemporary deformation of the Wasatch fault, Utah, from GPS measurements with implications for interseismic fault behavior and earthquake hazard: Observations and kinematic analysis: Journal of Geophysical Research, v. 111, p. B11405, doi: 10.1029/2006JB004326.

Colman, S.M., and Watson, K., 1983, Ages estimated from a diffusion equation model for scarp degradation: Science, v. 221, no. 4607, p. 263–265, doi: 10.1126/science.221.4607.263.

Coney, P.J., 1987, The regional tectonic setting and possible causes of Cenozoic extension in the North American Cordillera, *in* Coward, M.P., Dewey, J.F., and Hancock, P.L., eds., Continental Extensional Tectonics: Geological Society of London Special Publication 28, p. 177–186.

Coney, P.J., and Harms, T.A., 1984, Cordilleran metamorphic core complexes: Cenozoic extensional relics of Mesozoic compression: Geology, v. 12, p. 550–554, doi: 10.1130/0091-7613(1984)12<550:CMCCCE>2.0.CO;2.

Coogan, J.C., and DeCelles, P.G., 1996, Extensional collapse along the Sevier Desert reflection, northern Sevier Desert basin, western United States: Geology, v. 24, no. 10, p. 933–936, doi: 10.1130/0091-7613(1996)024<0933:ECATSD>2.3.CO;2.

Crone, A.J., 1983, Amount of displacement and estimated age of a Holocene surface faulting event, eastern Great Basin, Millard County, Utah, *in* Gurgel, K.D., ed., Geologic Excursions in Neotectonics and Engineering Geology in Utah: Boulder, Colorado, Geological Society of America, Rocky Mountain and Cordilleran Sections Meeting, Salt Lake City, Utah, Field Trip Guidebook, Part IV, p. 49–55.

Crone, A.J., Kyung, J., Machette, M.N., Lidke, D.J., Okumura, K., and Mahan, S.A., 2006, Data Related to Late Quaternary Surface Faulting on the Eastgate Fault, Churchill County, Nevada: U.S. Geological Survey Scientific Investigations Map 2893.

DeMets, C., and Dixon, T.H., 1999, New kinematic models for Pacific–North American motion from 3 Ma to present: I. Evidence for steady motion and biases in the NUVEL-1A model: Geophysical Research Letters, v. 26, p. 1921–1924, doi: 10.1029/1999GL900405.

dePolo, C.M., and Ramelli, A.R., 2003, The Warm Springs Valley fault system, a major right-lateral fault of the northern Walker Lane, western Nevada, *in* XVI International Union for Quaternary Research Congress: Paleoseismology in the Twenty-First Century, A Global Perspective: Reno, Nevada, International Union for Quaternary Research.

Dickinson, W.R., and Snyder, W.S., 1979, Geometry of subducted slabs related to San Andreas transform: The Journal of Geology, v. 87, p. 609–627, doi: 10.1086/628456.

Dixon, T.H., Robaudo, S., Lee, J., and Reheis, M.C., 1995, Constraints on present-day Basin and Range deformation from space geodesy: Tectonics, v. 14, no. 4, p. 755–772, doi: 10.1029/95TC00931.

Dixon, T.H., Miller, M., Farina, F., Wang, H., and Johnson, D., 2000, Present-day motion of the Sierra Nevada block and some tectonic implications for the Basin and Range Province, North American Cordillera: Tectonics, v. 1, p. 19–24.

Dohrenwend, J.C., Schell, B.A., and Moring, B.C., 1992, Reconnaissance Photogeologic Map of Young Faults in the Millett 1° by 2° Quadrangle, Nevada: U.S. Geological Survey Miscellaneous Field Studies Map MF-2176, 1:250,000.

Dohrenwend, J.C., Schell, B.A., Menges, C.M., Moring, B.C., and McKittrick, M.A., 1996, Reconnaissance Photogeologic Map of Young (Quaternary and Late Tertiary) Faults in Nevada: Nevada Bureau of Mines and Geology Open-File Report 96-2, 12 p., scale 1:250,000.

Doser, D.I., 1985, Source parameters and faulting processes of the 1959 Hebgen Lake, Montana, earthquake sequence: Journal of Geophysical Research, v. 90, p. 4537–4555, doi: 10.1029/JB090iB06p04537.

Doser, D.I., 1986, Earthquake processes in the Rainbow Mountain–Fairview Peak–Dixie Valley, Nevada, region 1954–1959: Journal of Geophysical Research, v. 91, p. 12,572–12,586, doi: 10.1029/JB091iB12p12572.

Eppes, M.C., McDonald, E.V., and McFadden, L.D., 2003, Soil geomorphological studies in the Mojave Desert: Impacts of Quaternary tectonics, climate, and rock type on soils, landscapes, and plant-community ecology, *in* Easterbrook, D.J., ed., Quaternary Geology of the United States: International Union for Quaternary Research 2003 Field Guide Volume, The Desert Research Institute, Reno, Nevada, p. 105–122.

Frankel, K.L., Brantley, D.S., Dolan, J.F., Finkel, R.C., Klinger, R.E., Knott, J.R., Machette, M.N., Owen, L.A., Phillips, F.M., Slate, J.L., and Wernicke, B.P., 2007a, Cosmogenic ^{10}Be and ^{36}Cl geochronology of offset alluvial fans along the northern Death Valley fault zone: Implications for transient strain in the Eastern California shear zone: Journal of Geophysical Research, v. 112, no. B6, p. B06407, doi: 10.1029/2006JB004350.

Frankel, K.L., Dolan, J.F., Finkel, R.C., Owen, L.A., and Hoeft, J.S., 2007b, Spatial variations in slip rate along the Death Valley–Fish Lake Valley fault system determined from LiDAR topographic data and cosmogenic ^{10}Be geochronology: Geophysical Research Letters, v. 34, no. 18, p. L18303, doi: 10.1029/2007GL030549.

Freymueller, J.T., Murray, M.H., Segall, P., and Castillo, D., 1999, Kinematics of the Pacific–North America plate boundary zone, northern California: Journal of Geophysical Research, v. 104, p. 7419–7441, doi: 10.1029/1998JB900118.

Friedrich, A.M., Lee, J., Wernicke, B.P., and Sieh, K., 2004, Geologic context of geodetic data across a Basin and Range normal fault, Crescent Valley, Nevada: Tectonics, v. 23, p. TC2015, doi: 10.1029/2003TC001528.

Gans, P.B., Mahood, G.A., and Schermer, E., 1989, Synextensional Magmatism in the Basin and Range Province: A Case Study from the Eastern Great Basin: Geological Society of America Special Paper 233, 53 p.

Gilbert, G.K., 1928, Studies of Basin and Range Structure: U.S. Geological Survey Professional Paper 153, 92 p.

Gile, L.H., Peterson, F.F., and Grossman, R.B., 1966, Morphological and genetic sequences of carbonate accumulation in desert soils: Soil Science, v. 101, no. 5, p. 347–360, doi: 10.1097/00010694-196605000-00001.

Haller, K.M., Machette, M.N., Dart, R.L., and Rhea, B.S., 2004, U.S. Quaternary fault and fold database released: Eos, v. 85, no. 22, p. 218, also at U.S. Geological Survey, http://geohazards.cr.usgs.gov/qfaults/index.html.

Hamilton, W., and Myers, W.B., 1966, Cenozoic tectonics of the western United States: Reviews of Geophysics, v. 4, p. 509–536, doi: 10.1029/RG004i004p00509.

Hammond, W.C., and Thatcher, W., 2004, Contemporary tectonic deformation of the Basin and Range Province, western United States: 10 years of observation with the Global Positioning System: Journal of Geophysical Research, v. 109, p. B08403, doi: 10.1029/2003JB002746.

Hammond, W.C., and Thatcher, W., 2005, Northwest Basin and Range tectonic deformation observed with the Global Positioning System, 1999–2003: Journal of Geophysical Research, v. 110, p. B10405, doi: 10.1029/2005JB003678.

Hammond, W.C., and Thatcher, W., 2007, Crustal deformation across the Sierra Nevada, northern Walker Lane, Basin and Range transition, western United States measured with GPS, 2000–2004: Journal of Geophysical Research, v. 112, p. B05411, doi: 10.1029/2006JB004625.

Hammond, W.C., Blewitt, G., Kreemer, C., Murray-Moraleda, J.R., and Svarc, J.L., 2010, GPS Constraints on Crustal Deformation before and during the 21 February 2008 Wells, Nevada, M 6.0 Earthquake, *in* The Wells, Nevada Earthquake Volume: NBMG/U.S. Geological Survey 2008 Wells, Nevada, Earthquake Report (in press).

Hanks, T.C., 2000, The age of scarplike landforms from diffusion-equation analysis, *in* Noller, J.S., Sowers, J.M, and Lettis, W.R., eds., Quaternary Geochronology: Methods and Applications: Washington, D.C., American Geophysical Union, Reference Shelf Volume 4, p. 313–337.

Hanks, T.C., and Andrews, D.J., 1989, Effect of far-field slope on morphologic dating of scarplike landforms: Journal of Geophysical Research, v. 94, p. 565–573, doi: 10.1029/JB094iB01p00565.

Hanks, T.C., and Wallace, R.E., 1985, Morphological analysis of the Lake Lahontan shoreline and beachfront fault scarps, Pershing County, Nevada: Bulletin of the Seismological Society of America, v. 75, p. 835–846.

Hanks, T.C., Bucknam, R.C., Lajoie, K.R., and Wallace, R.E., 1984, Modification of wave-cut and faulting-controlled landforms: Journal of Geophysical Research, v. 89, no. B7, p. 5771–5790, doi: 10.1029/JB089iB07p05771.

Harden, D.R., Biggar, N.E., and Gillam, M.L., 1985, Quaternary deposits and soils in and around Spanish Valley, Utah, *in* Weide, D.L., ed., Soils and Quaternary Geology of the Southwestern United States: Geological Society of America Special Paper 203, p. 48–65.

Harden, J.W., and Taylor, E.M., 1983, A quantitative comparison of soil development in four climatic regions: Quaternary Research, v. 20, p. 342–359, doi: 10.1016/0033-5894(83)90017-0.

Harden, J.W., Taylor, E.M., Reheis, M.C., and McFadden, L.D., 1991, Calcic, gypsic, and siliceous soil chronosequences in arid and semiarid environments, *in* Nettleton, W.D., ed., Occurrence, Characteristics, and Genesis of Carbonate, Gypsum, and Silica Accumulations in Soils: Soil Science Society of America Special Publication 26, p. 1–16.

Hecker, S., 1993, Quaternary Tectonics of Utah with Emphasis on Earthquake-Hazard Characterization: Utah Geological Survey Bulletin 127, 157 p.

Humphreys, E.D., 1995, Post-Laramide removal of the Farallon slab, western United States: Geology, v. 23, no. 11, p. 987–990, doi: 10.1130/0091-7613(1995)023<0987:PLROTF>2.3.CO;2.

Jackson, M.E., 1991, Paleoseismology of Utah: Volume 3. The Number and Timing of Holocene Paleoseismic Events on the Nephi and Levan Segments, Wasatch Fault Zone, Utah: Utah Geological Survey Special Studies 78, 23 p.

Jenny, H., 1941, Factors of Soil Formation: A system of quantitative pedology: New York, McGraw-Hill, 281 p.

Koehler, R.D., 2009, Late Pleistocene Regional Extension Rate Derived from Earthquake Geology of Late Quaternary Faults across Great Basin, Nevada between 38.5° and 40°N Latitude [Ph.D. thesis]: Reno, University of Nevada, 242 p.

Kreemer, C., Blewitt, G., and Hammond, W.C., 2009, Geodetic constraints on contemporary deformation in the Northern Walker Lane: 2. Velocity and strain rate tensor analysis, *in* Oldow, J.S., and Cashman, P.H., eds., Late Cenozoic Structure and Evolution of the Great Basin–Sierra Nevada Transition: Geological Society of America Special Paper 447, p. 17–31, doi: 10.1130/2009.2447(03).

Kurth, G.E., Phillips, F., Reheis, M., Redwine, J.L., and Paces, J., 2010, Cosmogenic nuclide and uranium-series dating of old, high shorelines in the western Great Basin, U.S.A.: Geological Society of America Bulletin (in press).

Lisiecki, L.E., and Raymo, M.E., 2005, A Pliocene-Pleistocene stack of 57 globally distributed benthic $\delta^{18}O$ records: Paleoceanography, v. 20, p. 1003, doi: 10.1029/2004PA001071.

Livaccari, R.F., Burke, K., and Sengor, A.M.C., 1981, Was the Laramide orogeny related to subduction of an oceanic plateau: Nature, v. 289, p. 276–278, doi: 10.1038/289276a0.

Machette, M.N., 1982, Guidebook to the Late Cenozoic Geology of the Beaver Basin, South Central Utah: U.S. Geological Survey Open-File Report 82–850, 42 p.

Machette, M.N., 1985a, Calcic soils of the southwestern United States, *in* Weide, D.L., ed., Soils and Quaternary Geology of the Southwestern United States: Geological Society of America Special Paper 203, p. 1–21.

Machette, M.N., 1985b, Late Cenozoic geology of the Beaver basin, southwestern Utah: Brigham Young University Geology Studies, v. 32, pt. 1, p. 19–37.

Machette, M.N., 1990, Temporal and spatial behavior of late Quaternary faulting, western United States, *in* Jacobson, J.L., ed., National Earthquake Hazards Reduction Program, Summaries of Technical Reports, Volume XXXI: U.S. Geological Survey Open-File Report 90–680, p. 438–440.

Machette, M.N., Personius, S.F., and Nelson, A.R., 1992, Paleoseismology of the Wasatch fault zone: A summary of recent investigations, interpretations, and conclusions, *in* Gore, P.L., and Hays, W.W., eds., Assessment of Regional Earthquake Hazards and Risk along the Wasatch Front, Utah: U.S. Geological Survey Professional Paper 1500-A-J, p. 1–54.

Machette, M.N., Haller, K.M., Ruleman, C.A., Mahan, S.A., and Okumura, K., 2005, Geologic Evidence for Late Quaternary Movement on the Clan Alpine Fault, West Central Nevada—Trench Logs, Scarp Profiles, Location Maps, and Sample and Soil Descriptions: U.S. Geological Survey Scientific Investigations Map 2891, version 1.0.

McCalpin, J., 1996, Paleoseismology: New York, Academic Press, 588 p.

McDonald, E.V., McFadden, L.D., and Wells, S.G., 2003, Regional response of alluvial fans to the Pleistocene-Holocene climatic transition, Mojave Desert, California, *in* Enzel, Y., Wells, S.G., and Lancaster, N., eds., Paleoenvironments and Paleohydrology of the Mojave and Southern Great Basin Deserts: Geological Society of America Special Paper 368, p. 189–205.

McFadden, L.D., 1982, The Impacts of Temporal and Spatial Climatic Changes on Alluvial Soils Genesis in Southern California [Ph.D. thesis]: Tucson, University of Arizona, 430 p.

Mifflin, M.D., and Wheat, M.M., 1979, Pluvial Lakes and Estimated Full Pluvial Climates of Nevada: Nevada Bureau of Mines and Geology Bulletin 94, 57 p.

Minster, J.B., and Jordan, T.H., 1987, Vector constraints on western U.S. deformation from space geodesy, neotectonics, and plate motions: Journal of Geophysical Research, v. 92, p. 4798–4804, doi: 10.1029/JB092iB06p04798.

Oviatt, C.G., 1989, Quaternary geology of part of the Sevier Desert, Millard County, Utah: Utah Geological and Mineral Survey Special Studies 70, 41 p., 1 pl., scale 1:100,000.

Oviatt, C.G., 1992, Quaternary Geology of the Scipio Valley Area, Millard and Juab Counties, Utah: Utah Geological Survey Special Studies 79, 16 p., scale 1:100,000.

Pancha, A., Anderson, J.G., and Kreemer, C., 2006, Comparison of seismic and geologic scalar moment rates across the Basin and Range Province: Bulletin of the Seismological Society of America, v. 96, no. 1, p. 11–32, doi: 10.1785/0120040166.

Piekarski, L.L., 1980, Relative age determination of Quaternary fault scarps along the southern Wasatch, Fish Springs, and House Ranges: Brigham Young University Geology Studies, v. 27, pt. 2, p. 123–139.

Pierce, K.L., and Colman, S.M., 1986, Effect of height and orientation (microclimate) on geomorphic degradation rates and processes, late glacial terrace scarps in central Idaho: Geological Society of America Bulletin, v. 97, no. 7, p. 869–885, doi: 10.1130/0016-7606(1986)97<869:EOHAOM>2.0.CO;2.

Ramelli, A.R., Bell, J.W., dePolo, C.M., and Yount, J.C., 1999, Large magnitude, late Holocene earthquakes on the Genoa fault, west-central Nevada and eastern California: Bulletin of the Seismological Society of America, v. 89, p. 1458–1472.

Ramelli, A.R., Bell, J.W., and dePolo, C.M., 2004, Peavine Peak: Another piece of the Walker Lane puzzle, *in* Lund, W.R., ed., Basin and Range Province: Seismic Hazards Summit: Reno, Nevada, Nevada Bureau of Mines and Geology, p. 126–127.

Redwine, J., 2003, The Quaternary Pluvial History and Paleoclimate Implications of Newark Valley, East-Central Nevada; Derived from Mapping and Interpretation of Surficial Units and Geomorphic Features [Master's thesis]: Arcata, California, Humboldt State University, 358 p.

Reheis, M., 1999, Extent of Pleistocene Lakes in the Western Great Basin: U.S. Geological Survey Miscellaneous Field Studies Map MF-2323, scale 1:800,000.

Reheis, M.C., 1987, Gypsic soils on the Kane alluvial fans, Big Horn County, Wyoming, *in* Harden, J.W., ed., Soil Chronosequences in the Western United States: U.S. Geological Survey Bulletin 1590-C, p. 1–39.

Reheis, M.C., and Sawyer, T.L., 1997, Late Cenozoic history and slip rates of the Fish Lake Valley, Emigrant Peak, and Deep Springs fault zones, Nevada and California: Geological Society of America Bulletin, v. 109, no. 3, p. 280–299, doi: 10.1130/0016-7606(1997)109<0280:LCHASR>2.3.CO;2.

Reheis, M.C., Slate, J.L., and Sawyer, T.L., 1995, Geologic Map of Late Cenozoic Deposits and Faults in Parts of the Mt. Barcroft, Piper Peak, and Soldier Pass 15′ Quadrangles, Esmeralda County, Nevada, and Mono County, California: U.S. Geological Survey Miscellaneous Investigations Series Map I-2264, scale 1:24,000.

Reheis, M.C., Slate, J.L., Throckmorton, C.K., McGeehin, J.P., Sarna-Wojcicki, A.M., and Dengler, L., 1996, Late Quaternary sedimentation on the Leidy Creek fan, Nevada-California: Geomorphic responses to climatic change: Basin Research, v. 8, p. 279–329, doi: 10.1046/j.1365-2117.1996.00205.x.

Reheis, M.C., Sarna-Wojcicki, A.M., Reynolds, R.L., Repenning, C.A., and Mifflin, M.D., 2002, Pliocene to Middle Pleistocene Lakes in the Western Great Basin: Ages and Connections, *in* Hershler, R., Madsen, D.B., and Currey, D.R., eds., Great Basin Aquatic Systems History: Washington, D.C., Smithsonian Contributions to the Earth Sciences, no. 33, Smithsonian Institution Press.

Sack, D., 1990, Geologic Map of the Tule Valley, West-Central Utah: Utah Geological and Mineral Survey Map 124, 26 p., pamphlet, scale 1:100,000.

Sarna-Wojcicki, A.M., and Davis, J.O., 1991, Quaternary tephrochronology, *in* Morrison, R.B., ed., Quaternary Nonglacial Geology: Conterminous U.S.: Boulder, Colorado, Geological Society of America, Geology of North America, v. K-2, p. 93–116.

Savage, J.C., Lisowski, M., Svarc, J.L., and Gross, K.K., 1995, Strain accumulation across the central Nevada seismic zone: Journal of Geophysical Research, v. 100, p. 20,257–20,269, doi: 10.1029/95JB01872.

Savage, J.C., Gan, W., Prescott, W.H., and Svarc, J.L., 2004, Stain accumulation across the Coast Ranges at the latitude of San Francisco, 1994–2000: Journal of Geophysical Research, B, Solid Earth and Planets, v. 109, no. 3, 11 p, doi:10.1029/2003JB002612.

Sawyer, T.L., 1990, Quaternary Geology and Neotectonic Activity along the Fish Lake Valley Fault Zone, Nevada and California [M.S. thesis]: Reno, University of Nevada, 379 p.

Schell, B.A., 1981, Faults and lineaments in the MX Siting Region, Nevada and Utah, Volume II: Technical Report to the U.S. Department of Defense, Air Force, Norton Air Force Base, California, under contract F04704–80-C-0006, 29 p., 11 pls., scale 1:250,000.

Schwartz, D.P., and Coppersmith, K.J., 1984, Fault behavior and characteristic earthquakes—Examples from the Wasatch and San Andreas fault zones: Journal of Geophysical Research, v. 89, no. B7, p. 5681–5698, doi: 10.1029/JB089iB07p05681.

Schwartz, D.P., Hanson, K.L., and Swan, F.H., III, 1983, Paleoseismic investigations along the Wasatch fault zone—An update, *in* Gurgel, K.D., ed., Geologic Excursions in Neotectonics and Engineering Geology in Utah, Guidebook—Part IV: Utah Geological and Mineral Survey Special Studies 62, p. 45–48.

Slate, J.L., 1992, Quaternary Stratigraphy, Geomorphology and Geochronology of Alluvial Fans, Fish Lake Valley, Nevada–California [Ph.D. thesis]: Boulder, University of Colorado, 241 p.

Sonder, L.J., and Jones, C.H., 1999, Western United States extension: How the West was widened: Annual Review of Earth and Planetary Sciences, v. 27, p. 417–462, doi: 10.1146/annurev.earth.27.1.417.

Sterr, H.M., 1985, Rates of change and degradation of hill slopes formed in unconsolidated materials—A morphometric approach to dating Quaternary fault scarps in western Utah, USA: Zeitschrift für Geomorphologie, v. 29, no. 3, p. 315–333.

Stewart, J.H., 1971, Basin and Range structure: A system of horsts and grabens produced by deep-seated extension: Geological Society of America Bulletin, v. 82, p. 1019–1044, doi: 10.1130/0016-7606(1971)82[1019:BARSAS]2.0.CO;2.

Stewart, J.H., 1978, Basin-Range structure in western North America: A review, *in* Smith, R.B., and Eaton, E.P., eds., Cenozoic Tectonics and Regional Geophysics of the Western Cordillera: Boulder, Colorado, Geological Society of America Memoir 152, p. 1–32.

Svarc, J.L., Savage, J.C., Prescott, W.H., and Murray, M.H., 2002b, Stain accumulation and rotation in western Nevada, 1993–2000: Journal of Geophysical Research, v. 107, doi: 10.1029/2001JB000579.

Taylor, E.M., 1989, Impact of Time and Climate on Quaternary Soils in the Yucca Mountain Area of the Nevada Test Site [M.S. thesis]: Boulder, Colorado, University of Colorado, 217 p.

Taylor, W.J., Bartley, J.M., Lux, D.R., and Axen, G.J., 1989, Timing of Tertiary extension in the Railroad Valley–Pioche transect, Nevada: Constraints from $^{40}Ar/^{39}Ar$ ages of volcanic rocks: Journal of Geophysical Research, v. 94, p. 7757–7774.

Thatcher, W., 2003, GPS constraints on the kinematics of continental deformation: International Geology Review, v. 45, p. 191–212, doi: 10.2747/0020-6814.45.3.191.

Thatcher, W., Foulger, G.R., Julian, B.R., Svarc, J.L., Quilty, E., and Bawden, G.W., 1999, Present-day deformation across the Basin and Range Province, western United States: Science, v. 283, p. 1714–1718, doi: 10.1126/science.283.5408.1714.

Treadwell-Steitz, C., and McFadden, L.D., 2000, Influence of parent material and grain size on carbonate coatings in gravelly soils, Palo Duro Wash, New Mexico: Geoderma, v. 94, p. 1–22, doi: 10.1016/S0016-7061(99)00075-0.

Wallace, R.E., 1977, Profiles and ages of young fault scarps, north-central Nevada: Geological Society of America Bulletin, v. 88, p. 1267–1281, doi: 10.1130/0016-7606(1977)88<1267:PAAOYF>2.0.CO;2.

Wallace, R.E., 1984a, Fault scarps formed during the earthquakes of October 2, 1915, in Pleasant Valley, Nevada, and some tectonic implications: U.S. Geological Survey Professional Paper, 1274-A, p. A1–A33.

Wallace, R.E., 1984b, Patterns and timing of late Quaternary faulting in the Great Basin Province and relation to some regional tectonic features: Journal of Geophysical Research, v. 89, p. 5763–5769, doi: 10.1029/JB089iB07p05763.

Wernicke, B.P., 1992, Cenozoic extensional tectonics of the Cordillera, U.S., *in* Burchfiel, B., Lipman, P., and Zoback, M., eds., The Cordilleran Orogen: Conterminous U.S.: Boulder, Colorado, Geological Society of America, The Geology of North America, v. G-3, p. 553–582.

Wernicke, B.P., Friedrich, A.M., Niemi, N.A., Bennett, R.A., and Davis, J.L., 2000, Dynamics of plate boundary fault systems from Basin and Range Geodetic Network (BARGEN) and geologic data: GSA Today, v. 10, no. 11, p. 1–7.

Wesnousky, S.G., Barron, A.D., Briggs, R.W., Caskey, J.S., Kumar, S., and Lewis, O., 2005, Paleoseismic transect across the northern Great Basin, USA: Journal of Geophysical Research, v. 110, p. BO5408, doi: 10.1029/2004JB003283.

Witkind, I.J., Weiss, M.P., and Brown, T.L., 1987, Geologic Map of the Manti 30′ × 60′ Quadrangle, Carbon, Emery, Juab, Sanpete, and Sevier Counties, Utah: U.S. Geological Survey Miscellaneous Investigations Map I-1631, scale 1:100,000.

Manuscript Received 17 June 2009
Revised Manuscript Received 21 January 2010
Manuscript Accepted 24 April 2010

Printed in the USA